The Meteoritical Society

Meteoritics & Planetary Science 45, Nr 12, 1906–1928 (2011)
doi: 10.1111/j.1945-5100.2010.01130.x

The Northwest Africa 1500 meteorite: Not a ureilite, maybe a brachinite

Cyrena Anne GOODRICH[1*], Noriko T. KITA[2], Michael J. SPICUZZA[2], John W. VALLEY[2], Jutta ZIPFEL[3], Takashi MIKOUCHI[4], and Masamichi MIYAMOTO[4]

[1]Planetary Science Institute, 1700 E. Ft. Lowell Road, Tucson, Arizona 85719, USA
[2]Wisc-SIMS, Department of Geoscience, University of Wisconsin, 1215 W. Dayton St., Madison, Wisconsin 53706, USA
[3]Forschungsinstitut und Naturmuseum Senckenberg, 60325 Frankfurt, Germany
[4]Department of Earth and Planetary Science, Graduate School of Science, University of Tokyo, 7-3-1 Hongo, Bunkyo-ku, Tokyo 113-0033, Japan
[*]Corresponding author. E-mail: cgoodrich@psi.edu

(Received 07 April 2010; revision accepted 28 August 2010)

Abstract–The Northwest Africa (NWA) 1500 meteorite is an olivine-rich achondrite containing approximately 2–3 vol% augite, 1–2 vol% plagioclase, 1 vol% chromite, and minor orthopyroxene, Cl-apatite, metal and sulfide. It was originally classified as a ureilite, but is currently ungrouped. We re-examined the oxygen three-isotope composition of NWA 1500. Results of ultra-high precision (~0.03‰ for $\Delta^{17}O$) laser fluorination analyses of two bulk chips, and high precision (~0.3‰) secondary ion mass spectrometry (SIMS) analyses of olivine and plagioclase in a thin section, show that the oxygen isotope composition of NWA 1500 ($\Delta^{17}O = -0.22$‰ from bulk samples and -0.18 ± 0.06‰ from 16 mineral analyses) is within the range of brachinites. We compare petrologic and geochemical characteristics of NWA 1500 with those of brachinites and other olivine-rich primitive achondrites, including new petrographic, mineral compositional and bulk compositional data for brachinites Hughes 026, Reid 013, NWA 5191, NWA 595, and Brachina. Modal mineral abundances, texture, olivine and pyroxene major and minor element compositions, plagioclase major element compositions, rare earth element abundances, and siderophile element abundances of NWA 1500 are within the range of those in brachinites and, in most cases, well distinguished from those of winonaites/IAB silicates, acapulcoites/lodranites, ureilites, and Divnoe. NWA 1500 shows evidence of internal reduction, in the form of reversely zoned olivine (Fo ~65–73 core to rim) and fine-grained intergrowths of orthopyroxene + metal along olivine grain margins. The latter also occur in Reid 013, Hughes 026, NWA 5191, and NWA 595. We argue that reduction (olivine $\rightarrow$ enstatite + Fe^0 + O_2) is the best hypothesis for their origin in these samples as well. We suggest that NWA 1500 should be classified as a brachinite, which has implications for the petrogenesis of brachinites. Fe-Mn-Mg compositions of brachinite olivine provide evidence of redox processes among bulk samples. NWA 1500 provides evidence for redox processes on a smaller scale as well, which supports the interpretation that these processes occurred in a parent body setting. SIMS data for ^{26}Al-^{26}Mg isotopes in plagioclase in NWA 1500 show no ^{26}Mg excesses beyond analytical uncertainties (1–2‰). The calculated upper limit for the initial $^{26}Al/^{27}Al$ ratio of the plagioclase corresponds to an age younger than 7 Ma after CAI. Compared to ^{53}Mn-^{53}Cr data for Brachina (Wadhwa et al. 1998b), this implies either a much younger formation age or a more protracted cooling history. However, Brachina is atypical and this comparison may not extend to other brachinites.

INTRODUCTION

Northwest Africa (NWA) 1500 is an augite-bearing, olivine-rich achondrite that is currently classified as ungrouped (Meteoritical Bulletin Database). It was initially classified as a main-group[1] ureilite, albeit with several rare or unusual characteristics (Bartoschewitz et al. 2003; Russell et al. 2003). In particular, NWA 1500 contains plagioclase, which does not occur in any main-group ureilite, and for this reason was heralded by Bartoschewitz et al. (2003) as the first basaltic ureilite. However, Mittlefehldt and Hudon (2004) argued that too many of the mineral and bulk compositional characteristics of this meteorite are out of the ureilite range for it to be a ureilite at all. Goodrich et al. (2006) carried out a detailed petrologic and geochemical study of NWA 1500, and compared it to the augite-bearing ureilites. The conclusion of this work was that although NWA 1500 might have been derived from a previously unsampled part of the ureilite parent body (UPB), there were many difficulties with such a model. Ultimately, Goodrich et al. (2006) accepted the conclusion of Mittlefehldt and Hudon (2004) that NWA 1500 should be considered ungrouped, but suggested that the parent body from which this meteorite was derived may have had a differentiation history similar to that of the UPB.

Oxygen isotope compositions can be used as a parent body signature. The first oxygen isotope data reported for NWA 1500 (Bartoschewitz et al. 2003; Russell et al. 2003) showed a single bulk analysis to be intermediate between the field of winonaites/IAB silicates and that of acapulcoites/lodranites on a standard oxygen three-isotope plot, considerably out of the range of oxygen isotope compositions of ureilites (Fig. 1). Mittlefehldt and Hudon (2004) regarded these data as evidence that NWA 1500 is not a ureilite. By contrast, Bartoschewitz et al. (2003) and Goodrich et al. (2006) were more compelled by the possibility of a petrologic relationship between NWA 1500 and ureilites, and chose not to accept this conclusion a priori. The inference that NWA 1500 may have been derived from a second parent body with UPB-like characteristics (Goodrich et al. 2006) brought new significance to its apparently unique oxygen isotope composition.

To clarify the classification and petrogenesis of NWA 1500, we began a re-examination of its bulk and internal oxygen isotope variation. While our work was in progress, new oxygen isotope data for NWA 1500 were reported in an abstract by Greenwood et al. (2007).

[1]The term "main-group" refers to those ureilites previously referred to as "monomict." See discussion in Downes et al. (2008) and Goodrich et al. (2009).

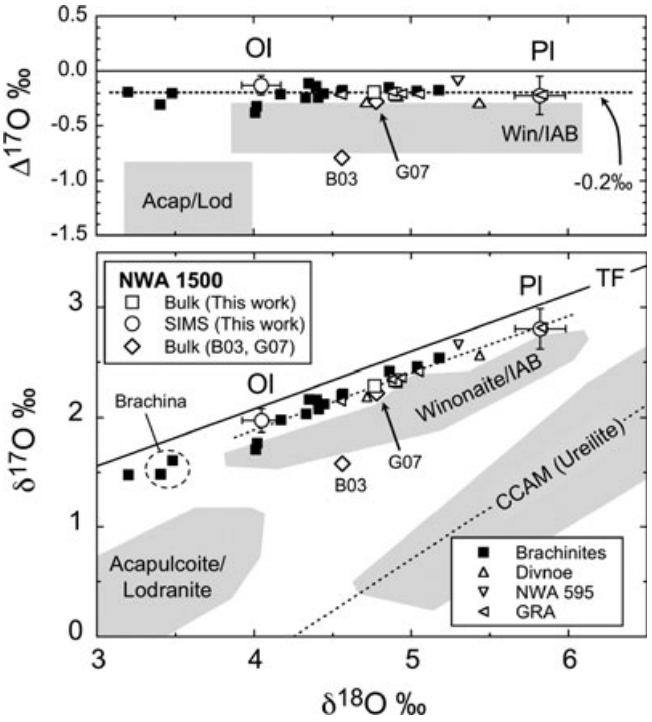

Fig. 1. Oxygen three isotope ratios of NWA 1500. Upper and lower figures show plots of $\delta^{18}O$ versus $\Delta^{17}O$ and $\delta^{17}O$, respectively. Open squares and circles are bulk laser fluorination data and SIMS data, respectively. "Ol" and "Pl" indicate the average values of SIMS olivine and plagioclase analyses. Literature data for bulk NWA 1500 are shown as diamonds, labeled "B03" (Bartoschewitz et al. 2003) and "G07" (Greenwood et al. 2007). "TF" and "CCAM" indicate the terrestrial mass fractionation line and the carbonaceous chondrite anhydrous mineral line (Clayton et al. 1977). Filled squares are bulk brachinite data from Clayton and Mayeda (1996), Irving et al. (2005), Irving and Rumble (2006), Rumble et al. (2008) and Greenwood et al. (2007). Data for NWA 595 (Irving et al. 2005) and Divnoe (Rumble et al. 2008; Greenwood et al. 2007) shown for comparison. Also shown are data for GRA 06128/06129 (GRA), a sodic plagioclase-dominated meteorite that may be related to brachinites (Ziegler et al. 2008; Day et al. 2009; Shearer et al. 2010). The gray fields are for other groups of primitive achondrites (Clayton and Mayeda 1996), as labeled. Note that the ureilite field extends along the CCAM line to $\delta^{18}O = \sim 8.5$. Bulk and SIMS oxygen isotope data for NWA 1500 plot within the range of brachnites, Divnoe, NWA 595 and GRA ($\Delta^{17}O = \sim -0.2‰$), and are distinguished from ureilites, acapulcoites/lodranites and winonaites/IAB silicates.

These data showed a bulk composition very different from that of the original data (Fig. 1)—one that is within the range of brachinites and several other ungrouped achondrites, and thus raises a new set of questions about the origin of this meteorite. Here, we report results of ultra-high precision (~0.03‰ for $\Delta^{17}O$) laser fluorination analyses of two bulk chips, and high precision (~0.3‰) secondary ion mass spectrometry (SIMS) analyses of

individual minerals in a thin section, of NWA 1500. These results confirm that the oxygen isotope composition of NWA 1500 is within the range of brachinites. Therefore, we compare petrologic and geochemical characteristics of NWA 1500 with those of brachinites and several possibly related ungrouped achondrites, including new data we have obtained for Hughes 026, Reid 013, NWA 5191, and NWA 595. In addition, we carried out a SIMS study of ^{26}Al-^{26}Mg isotopes in plagioclase in a thin section of NWA 1500, for comparison with published chronological data for brachinites. We discuss the question of whether NWA 1500 should be classified as a brachinite, and implications of doing so for various aspects of brachinite petrogenesis.

SAMPLES AND ANALYTICAL TECHNIQUES

Oxygen Isotope Analyses Using Laser Fluorination Mass Spectrometer

Oxygen three-isotope analyses of bulk chips of NWA 1500 were conducted in the Stable Isotope Laboratory at the University of Wisconsin, Madison (Spicuzza et al. 2007). Two chips of NWA 1500, weighing approximately 2.5 mg each, were analyzed using the laser fluorination extraction line and Finnigan MAT 251 mass spectrometer. International Garnet standard UWG-2 ($\delta^{18}O = 5.80‰$ VSMOW; Valley et al. 1995) was analyzed before and after the NWA 1500 sample measurements. The terrestrial mass fractionation correction law of $(1 + \delta^{17}O/1000) = (1 + \delta^{18}O/1000)^{\lambda}$ with $\lambda = 0.5259$ was applied following Spicuzza et al. (2007) who determined $\delta^{17}O = 3.046‰$ for UWG-2. The deviation from the terrestrial mass fractionation line, $\Delta^{17}O$, is expressed as $\Delta^{17}O = 1000 \times [\ln(1 + \delta^{17}O/1000) - 0.5259 \times \ln(1 + \delta^{18}O/1000)]$. Long-term reproducibility of the UWG-2 standard by laser fluorination (2SD; standard deviation) is 0.10‰, 0.10‰, and 0.03‰ for $\delta^{18}O$, $\delta^{17}O$, and $\Delta^{17}O$, respectively. Due to the low degree of terrestrial weathering of NWA 1500 (Goodrich et al. 2006), acid leaching was not applied to the bulk samples.

Oxygen and Al-Mg Isotope Analyses Using SIMS

The SIMS oxygen three-isotope and Al-Mg analyses were carried out at WiscSIMS with an IMS-1280 ion microprobe on section #r1 of NWA 1500, which contains a vein with several large (~1–2 mm) poikilitic plagioclase (~An_{37}) grains (Goodrich et al. 2006). Oxygen isotope analyses were performed on olivine and plagioclase using three Faraday Cup detectors and methods similar to those of Kita et al. (2009, 2010). The Cs^+ primary beam was focused to 15μm diameter with intensity of 6 nA. We used a thin section of San Carlos olivine as a running standard. Three plagioclase standards (An_{22}-An_{49}) were used to calibrate instrumental bias between analyses of olivine and plagioclase. The typical external reproducibility of the olivine standard was 0.3–0.4‰ for $\delta^{18}O$ and $\delta^{17}O$. For SIMS analyses of meteoritic samples, the mass fractionation correction law assumes $\lambda = 0.52$ according to Clayton et al. (1991) and $\Delta^{17}O$ is defined as $\Delta^{17}O = \delta^{17}O - 0.52 \times \delta^{18}O$. The external reproducibility of the olivine standard was better than 0.3‰ for $\Delta^{17}O$ values. Systematic differences caused by using a different mass fractionation law than that used for the bulk ultra-high precision laser fluorination analyses are small compared to the analytical uncertainties of the SIMS or laser fluorination analyses. A detailed data table including measurements of the standards is given in Table S1 (Supporting Information).

The Al-Mg isotope analyses were carried out on the large plagioclase grains in the vein in the same thin section. The analytical conditions were similar to those in Kita et al. (2000, 2003a). The O^- primary beam was adjusted to approximately 10×20 μm oval shape with intensity of 1–2 nA. Mineral and glass standards with labradorite composition were used for calibrating Al/Mg ratios and Mg isotope analyses. The secondary $^{24}Mg^+$ intensities were in the range from 4×10^4 to 2.7×10^5 cps for standards, whereas those in NWA 1500 plagioclase were $(3–7) \times 10^4$ cps. The three Mg isotopes were detected using the mono-collector electron multiplier (EM) in pulse counting mode with magnetic peak switching. The $^{27}Al^+$ signals were obtained simultaneously with $^{25}Mg^+$ using a multicollector Faraday Cup on the high mass side. The dead time of the EM detector was 23 ns. A single spot analysis typically took 1 h, including 100 cycles of Mg isotope measurements. The external reproducibility of mass fractionation corrected $\delta^{26}Mg$ in glass standards with Mg contents similar to those of plagioclase in NWA 1500 was approximately 1–2‰. The external reproducibility of measured $^{27}Al/^{24}Mg$ ratios of plagioclase standards is better than 1%, although the accuracy of corrected $^{27}Al/^{24}Mg$ ratios is at the level of 10% due to uncertainties of Mg contents in the standards. A detailed data table including measurements of the standards is given in Table S2.

Scanning Electron Microscopy and Electron Microprobe Analysis

We studied three thin sections of Reid 013/Nova 003 (AMNH sections 4815-1, 4815-4, and 4815-5), one thin section of Hughes 026 (AMNH 4883-2), one thin

section of Brachina (AMNH section 4489-1), one thin section of NWA 595 (UCLA), and one thick section of NWA 5191 (Museo Nazionale dell''Antartide). We also re-examined section #1 of NWA 1500 (see Goodrich et al. 2006). Backscattered electron images were obtained using the Zeiss EVO50 XVP scanning electron microscope (SEM) in the Department of Geosciences at the University of Massachusetts, Amherst. Electron microprobe analyses of Reid 013/Nova 003 and Hughes 026 were carried out using the JEOL JXA 8900RL at Johannes Gutenberg Universität in Mainz under conditions described in Goodrich and Righter (2000). Analyses of NWA 595 and NWA 5191 were carried out with the Cameca SX-50 electron microprobe at the University of Massachusetts. High precision analyses of olivine were obtained using 15 keV accelerating potential and 60 nA beam current, with counting times of 300–400 s for Mn, Cr and Ca, and 40 s for Mg, Fe and Si. Olivines in three brachinites previously analyzed under similar conditions (Goodrich and Righter 2000) were analyzed at the same time (Brachina—7 analyses; Reid 013—9 analyses; and Hughes 026—8 analyses) to test for consistency with the previous data set. These tests showed Cr_2O_3, CaO, MgO, and FeO contents within error of previous values, although MgO was systematically low by 1–3% and FeO was systematically high by 1%. By contrast, MnO contents were not within error of previous values, and were lower by 4.5–5.5% relative. We therefore checked our Mn calibration by analyzing a sample of San Carlos olivine. Results of 10 analyses gave a value of 0.127 ± 0.003 wt% MnO, which is within error of that published by Ito and Ganguly (2006) for San Carlos olivine but lower than the official value (0.14% MnO, based on a wet-chemical analysis) for the San Carlos olivine standard (USNM 111312/444) used by Goodrich and Righter (2000). It is not possible to determine which of these sets of analyses is more accurate. However, as our principle interest is in having a self-consistent set of high precision data, we simply corrected our analyses of olivine in NWA 595 and NWA 5191 (MgO: +2% relative; FeO: −1% relative; MnO: +5% relative) to make them consistent with the data of Goodrich and Righter (2000). Conditions for analyses of pyroxenes were 15 keV accelerating potential and 30 nA beam current, with 10–30 s counting times.

Modal abundances of phases in Reid 013, Hughes 026, NWA 5191, and NWA 595 were determined by point-counting collages of backscattered electron images of whole thin sections, combined with SEM and optical microscopy to ensure accurate identification of each phase.

Table 1. Bulk laser fluorination oxygen isotope analyses of NWA 1500.

Sample	mg	$\delta^{18}O$ (‰)	$\delta^{17}O$ (‰)	$\Delta^{17}O$ (‰)[a]
WR chip-1	2.77	4.77	2.29	−0.21
WR chip-2	2.43	4.90	2.34	−0.23
Average		4.83	2.32	−0.22

[a]For definition of $\Delta^{17}O$, see text.

Neutron Activation Analysis

Bulk samples of Hughes 026 (one 174.13 mg rock chip) and of Reid 013 (two rock chips of 188.02 and 179.35 mg, respectively) were provided by Mini Wadhwa from the Field Museum in Chicago. Neutron activation analyses were carried out at Max-Planck-Institut für Chemie in Mainz. Samples were irradiated for 6 h under a thermal neutron flux of 7×10^{11} n cm^{-2} s^{-1} at the TRIGA Mark II Reactor of the Institut für Kernchemie at the Johannes Gutenberg-Universität in Mainz. After irradiation, samples were repeatedly counted over several weeks on Ge(Li) and Hp-Ge detectors at the Max-Planck-Institut. Counting times ranged from 30 min directly after end of irradiation, to several days 3–4 weeks later. The SD errors given are 1σ standard deviations from a mean and include errors from counting statistics, counting geometries, counting reproducibility, and variations in neutron flux. Preliminary results of these analyses were published by Wadhwa et al. (1998a).

RESULTS

Oxygen Isotopes

Results of bulk (laser fluorination) and in situ (SIMS) oxygen three-isotope analyses are shown in Tables 1 and 2, respectively, and plotted in Fig. 1. The two bulk analyses show the average values of $\delta^{18}O = 4.8‰$, $\delta^{17}O = 2.3‰$, and $\Delta^{17}O = -0.22‰$, which are significantly different from the analysis reported by Bartoschewitz et al. (2003). The new bulk data are consistent with the analysis of NWA 1500 by Greenwood et al. (2007), and within the range of bulk oxygen isotope compositions of brachinites, NWA 595, Divnoe, and GRA 06128/06129 (Fig. 1). The reason for the discrepancy between these data and the analysis reported by Bartoschewitz et al. (2003) is not clear.

The SIMS oxygen three-isotope data from olivine and plagioclase in NWA 1500 plot on a mass dependent fractionation line that passes through the bulk data, at lower and higher $\delta^{18}O$, respectively (Fig. 1). The average $\Delta^{17}O$ value for all the SIMS analyses gives $\Delta^{17}O = -0.18 \pm 0.06‰$, indistinguishable from that of

Table 2. SIMS oxygen three-isotope analyses of olivine and plagioclase in NWA 1500[a].

SIMS analysis spot (mineral-analysis number)	$\delta^{18}O$ (‰)	$\delta^{17}O$ (‰)	$\Delta^{17}O$ (‰)[b]
Olivine-1 (core[c])	3.93 ± 0.40	1.95 ± 0.25	−0.11 ± 0.19
Olivine-2	4.42 ± 0.40	2.07 ± 0.25	−0.24 ± 0.19
Olivine-3 (core)	4.22 ± 0.40	2.13 ± 0.25	−0.08 ± 0.19
Olivine-4 (core)	4.23 ± 0.40	2.24 ± 0.25	0.03 ± 0.19
Olivine-5 (core)	4.23 ± 0.40	1.97 ± 0.25	−0.24 ± 0.19
Olivine-6 (core)	4.09 ± 0.40	1.98 ± 0.25	−0.16 ± 0.19
Olivine-7	3.99 ± 0.40	1.74 ± 0.25	−0.35 ± 0.19
Olivine-13 (core)	3.70 ± 0.37	1.55 ± 0.35	−0.38 ± 0.30
Olivine-14 contact with pyroxene	3.94 ± 0.37	1.76 ± 0.35	−0.29 ± 0.30
Olivine-15 (core)	3.94 ± 0.37	2.15 ± 0.35	0.10 ± 0.30
Olivine-16 (rim)	3.84 ± 0.37	1.79 ± 0.35	−0.21 ± 0.30
Plagioclase PL3-8	5.90 ± 0.37	2.73 ± 0.35	−0.36 ± 0.30
Plagioclase PL1-9	5.92 ± 0.37	2.72 ± 0.35	−0.37 ± 0.30
Plagioclase PL1-10	5.86 ± 0.37	2.84 ± 0.35	−0.23 ± 0.30
Plagioclase PL2-11	5.87 ± 0.37	2.96 ± 0.35	−0.11 ± 0.30
Plagioclase PL2-12	5.72 ± 0.37	2.85 ± 0.35	−0.14 ± 0.30
Average olivine (n = 11)[d]	4.05 ± 0.13	1.94 ± 0.13	−0.17 ± 0.07
Average plagioclase (n = 5)[d]	5.86 ± 0.17	2.82 ± 0.16	−0.24 ± 0.14
All data (n = 16)[d]			−0.18 ± 0.06

[a]Full analytical data including standards are given in Table S1. Uncertainties assigned to each datum are external reproducibility (2SD) of the olivine standard.
[b]Calculated as $\Delta^{17}O = \delta^{17}O - 0.52 \times \delta^{18}O$.
[c]"Core" and "rim" refer to olivine grain with reverse zonation.
[d]Mean values and 2 standard deviations (2SD) are calculated for $\delta^{18}O$ and $\delta^{17}O$. Weighted averages and errors are calculated for $\Delta^{17}O$.

Table 3. Al-Mg isotope analyses of plagioclase in NWA 1500.

Analysis spot	$^{27}Al/^{24}Mg$[a]	$\delta^{26}Mg$[b]
PL1 #3	1097	−1.3 ± 1.0
PL1 #4	1038	1.0 ± 1.4
PL1 #5	1031	1.1 ± 1.9
PL1 #6	1036	0.5 ± 2.2
PL2 #1	1012	0.7 ± 1.4
PL2 #2	999	−0.1 ± 1.4
PL2 #3	1057	0.8 ± 2.1
PL2 #4	1023	−0.5 ± 2.0
PL2 #5	1031	−0.7 ± 2.2
PL3 #1	1026	0.3 ± 1.4
PL3 #2	1026	−0.8 ± 2.1
All data (n = 11)	1034 ± 15	0.0 ± 0.5[c]

[a]External reproducibility of the plagioclase standard is better than 1% and the accuracy of the calibration is approximately 10%.
[b]Errors assigned to each datum are at 95% confidence level including uncertainty of standard analyses.
[c]Weighted average.

the bulk analyses (−0.22 ± 0.03‰). Multiple analyses of olivine and plagioclase showed reproducibility similar to that of the running standard analyses, indicating that the individual minerals in NWA 1500 are homogeneous in $\delta^{18}O$ and $\delta^{17}O$ to better than 0.4‰. The difference in $\delta^{18}O$ between olivine and plagioclase (An_{37}) is calculated from the average values in Table 2 to be $\delta^{18}O$ (pl-ol) = 1.8 ± 0.2‰. The oxygen isotope equilibrium temperature is calculated to be 870 ± 70 °C by applying the reduced partition function for forsterite, anorthite, and albite (Clayton and Kieffer 1991; see Table S3 for calculation). As discussed below, this temperature is in agreement with pyroxene equilibration temperatures for NWA 1500 (Goodrich et al. 2006).

^{26}Al-^{26}Mg Isotopes

Results of the SIMS Al-Mg isotope analyses of plagioclase are shown in Table 3. The $^{27}Al/^{24}Mg$ ratios in the plagioclase grains are constant within ±5% at a value of approximately 1000. None of the data show distinguishable ^{26}Mg excess beyond the analytical uncertainties (1–2‰). The average of 11 analyses yield $\delta^{26}Mg = 0.0 \pm 0.5$‰. The upper limit for the model initial $^{26}Al/^{27}Al$ ratio of the plagioclase is calculated to be $< 6 \times 10^{-8}$, corresponding to an age younger than 7 Myr after calcium-aluminum-rich inclusion (CAI) formation assuming initial $^{26}Al/^{27}Al = 5.2 \times 10^{-5}$ (Jacobsen et al. 2008).

NWA 1500: Petrography and Mineral Compositions

The following description is based on Mittlefehldt and Hudon (2004) and Goodrich et al. (2006),

Table 4. Petrographic characteristics of NWA 1500, brachinites, and other ungrouped olivine-rich achondrites.

	Modal abundance (vol%)										
	Olivine	Augite	opx	Plagioclase	Phosphate	Chromite	Metal[d]	Sulfide	Fo	Olivine grain size (mm)	Ref.
NWA 1500 (ungrouped)	95–96	1.7–3.1	Minor	0.3–1.8	Minor	0.6–1.6	Trace	Trace	65–73	0.1–0.5	1
Brachina	80.4	5.5	Trace	9.9	0.5	0.5	Trace	3.2	69–70	0.1–0.3	2,3,4
EET 99402/99407	85–87	4–5	None	6.3–9.1	Trace	0.6–0.9	Trace	0.1–1	64.2	0.5–1.5	5
Reid 013/Nova 003[a]	≥96	Trace-1	Yes	Trace-3		Minor	Trace	Trace	66.8	Bimodal (<0.2,0.5)	4,6,7
Reid 027	Yes	Yes	Yes	Abundant	Yes	Yes	Yes	Yes	65.3	0.1–0.6	8
NWA 4876	90	5		2		<3	<3	<3	66.6	0.02–1.4	9
NWA 4969	89	6	None	2.5		1.5	<1	<1	65	Bimodal (0.1, 1)	9,10
NWA 4874	90	4	None	2	1	3	1		65	Avg. 0.7	9,10
NWA 4882	85–90	Yes	None	Yes		Yes	Yes	Yes	65	Avg. 0.7	9,10
ALH 84025	79–90	4–15	None	None	Trace	0.8–2	<1%	3–4	67–68	Max. 1.8; Avg. 0.7	4,5,11
Eagle's Nest	81	6	None	None	Trace	<2		7	68	Max. 1.5	12,13
Hughes 026[b]	92.7	3.6	1.6	<0.1	0.1	0.8	<0.1	1.2		0.65	4,7,14
NWA 3151[c]	95	Minor	Rare	Rare		Yes	Yes	Yes	64.3	0.7–1.6	15,16
NWA 5191[c]	90	7	Minor	None		1–2	Trace	Trace	66.4	0.1–1 (Avg. 0.4)	7
NWA 4872	85	3	None	None	3	5	2	2	65	Bimodal (0.1, 1)	9,10
NWA 595 (ungrouped?)	80	5–10	10–15	None		Minor	Trace	Trace	71–72		15,16
	90	3	6.5	None		Minor	Trace	Trace	71.7	0.5–3	7
Divnoe (ungrouped)	74.6	.....14.3.....		1.5	Yes	.....9.5 (opaques).....			72–80	0.3–1	18

[a]Formerly called Window Butte.

[b]Formerly called Australia I.

[c]It has been suggested [19] that NWA 5191 and NWA 3151 are paired; our work on NWA 5191 suggests that this needs further investigation.

[d]Metal or Fe-oxides assumed to be alteration products of metal.

References: [1] Goodrich et al. (2006); [2] Nehru et al. (1983); [3] Smith et al. (1983); [4] Goodrich and Righter (2000); [5] Mittlefehldt et al. (2003); [6] Wlotzka (1993b); [7] This work; [8] Grossman (1998); [9] Connolly et al. (2008); [10] Rumble et al. (2008); [11] Warren and Kallemeyn (1989); [12] Kring et al. (1991); [13] Swindle et al. (1998); [14] Nehru et al. (1996); [15] Connolly et al. (2006); [16] Irving et al. (2005); [17] Russell et al. (2002); [18] Petaev et al. (1994). [19] Weisberg et al. (2008).

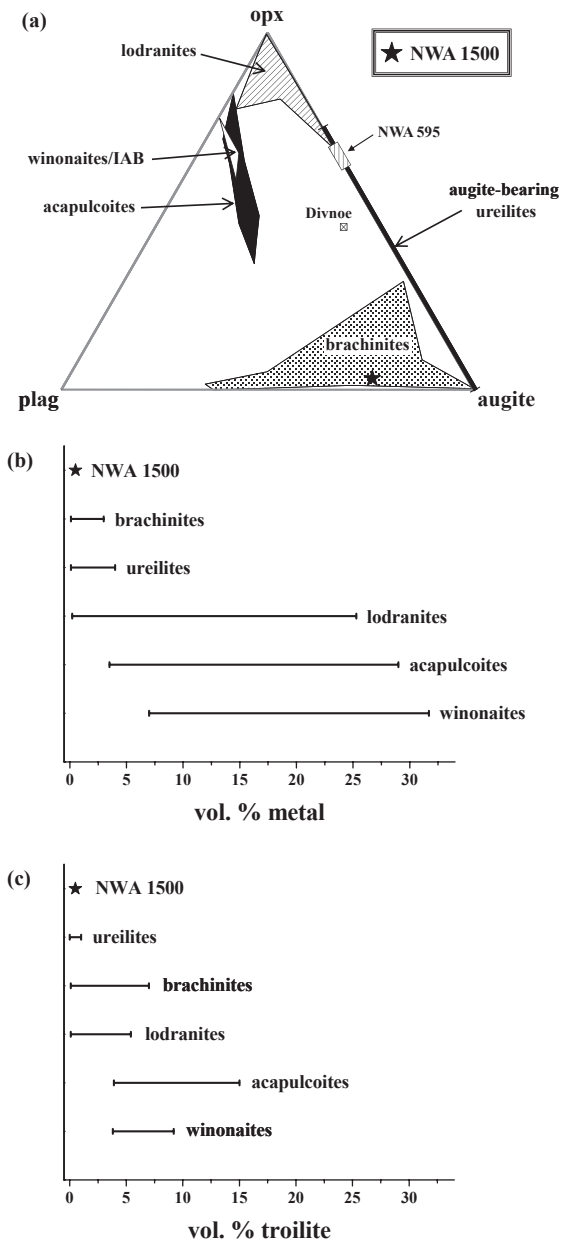

Fig. 2. Modal abundances in NWA 1500, brachinites, and other olivine-rich primitive achondrites. a) Ternary diagram showing relative abundances of the major silicate phases other than olivine (plagioclase, augite, orthopyroxene) in olivine-rich primitive achondrites. NWA 1500 has modal abundances within the range of brachinites and well distinguished from other groups. b) Abundances of metal. c) Abundances of troilite. Sources of data as follows. NWA 1500: Goodrich et al. (2006). Brachinites: Nehru et al. (1983); Smith et al. (1983); Warren and Kallemeyn (1989); Mittlefehldt et al. (2003); Swindle et al. (1998); Kring et al. (1991); Wlotzka (1993b); Grossman (1998); Connolly et al. (2006, 2008). Acapulcoites: McCoy et al. (1996); Patzer et al. (2004); Burroni and Folco (2008); Yugami et al. (1998). Lodranites: Takeda et al. (1994); Papike et al. (1995). Winonaites and IAB silicates: Yugami et al. (1998). NWA 595: Connolly et al. (2006). Divnoe: Petaev et al. (1994). Ureilites: Mittlefehldt et al. (1998).

supplemented by new observations. NWA 1500 consists of ≥95% olivine, 2–3% augite, 1–2% plagioclase, 0.5–1.5% chromite (all vol%), and minor orthopyroxene, Cl-apatite, metal, and sulfide (Table 4; Fig. 2). Olivine-rich areas have an "equilibrated" texture with triple junctions and rounded grain boundaries (Fig. 3a), and show a weak preferred orientation. Typical olivine grain size is approximately 0.1–0.5 mm. Augite grains range to larger sizes (~1 mm) and are commonly intergranular. Plagioclase occurs principally in vein-like areas as large poikilitic grains (up to ~3 mm) enclosing rounded olivine and augite grains, and elsewhere as rare patches of smaller (<25 μm), interstitial grains. The vein-like areas also have concentrations of augite and orthopyroxene. The latter occurs as interstitial grains and overgrowths on olivine, often containing small islands of olivine that suggest formation by the reaction olivine + melt → orthopyroxene (opx1; Fig. 4a).

Olivine major and minor element compositions are shown in Figs. 5–7. Olivine core compositions range from Fo 65 to 72, with a strong peak at Fo 68–69. Most grains are reverse-zoned from Fo ~68 or 69 to Fo ~73. Rare grains are reverse-zoned from Fo ~65 to 73. In most cases, the outermost rims (~10–30 μm) show a steeper zonation profile and may contain tiny grains of metal. These rims are similar to the "reduction rims" that are characteristic of ureilite olivine (Wlotzka 1972; Goodrich 1992; Mittlefehldt et al. 1998), although they contain significantly less metal than in ureilites. All olivine compositions plot along a single redox trend on a plot of molar Fe/Mg versus Fe/Mn (Fig. 5). Almost all olivine-olivine grain boundaries are lined with fine-grained assemblages of orthopyroxene + opaque phases (Fig. 3a). This material also occurs along olivine-augite and olivine-chromite grain boundaries and as veins within olivine, and is texturally distinct from the olivine "reduction rims." The opaques in these assemblages are dominantly Fe-oxides, with lesser sulfide and rare metal. Bartoschewitz et al. (2003) reported that grain boundary areas contain finely dispersed graphite. However, Mittlefehldt and Hudon (2004) reported that the bulk carbon content of NWA 1500 was below detection limits and Goodrich et al. (2006) reported that graphite occurred only rarely. We re-examined those occurrences and find that they cannot be unambiguously distinguished from cracks containing accumulated carbon coat. Thus, it is not certain that there is any graphite in NWA 1500.

Pyroxene major and minor element compositions are shown in Figs. 7 and 8. Augite is homogeneous Wo 45, *mg* (= 100 × molar Mg/[Mg + Fe]) 80.6. Orthopyroxene in the vein-like areas (opx1; Fig. 4a) is Wo 2.1, *mg* ~71 while that in the grain boundary (opx + opaques) assemblages (opx2; Fig. 4a) is

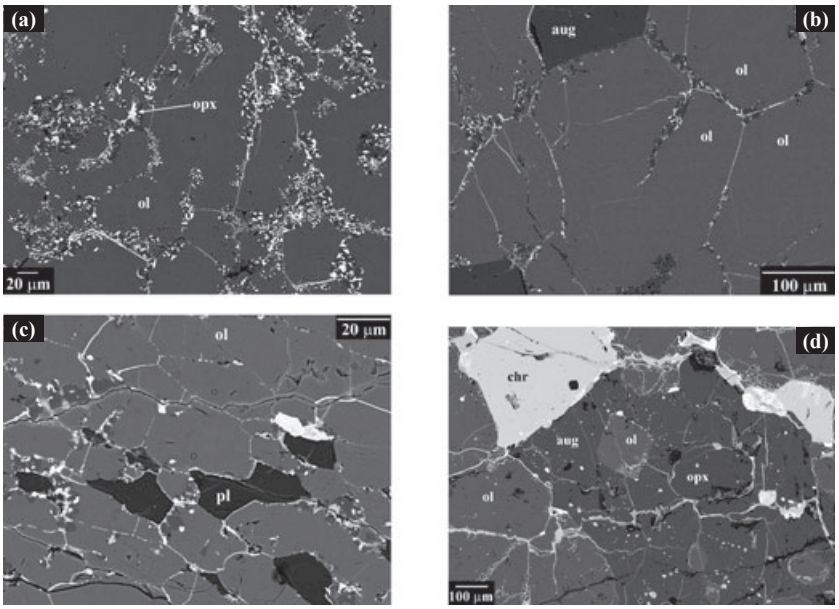

Fig. 3. Backscattered electron images (BEI) of NWA 1500 and possibly related meteorites studied here. a) NWA 1500. Olivine, with grain boundaries lined by fine-grained assemblages of orthopyroxene + opaque phases. Note common triple junctions. Olivine grains are weakly reverse-zoned (difficult to see at contrast shown). b) Brachinite Hughes 026. Olivine (note triple junctions) and augite. Grain boundaries lined by fine-grained assemblages of orthopyroxene + opaque phases. c) Brachinite Reid 013. Vein-like area having higher abundance of plagioclase and finer-grain size than bulk rock. d) NWA 595, showing coarse poikilitic augite enclosed rounded olivine and orthopyroxene.

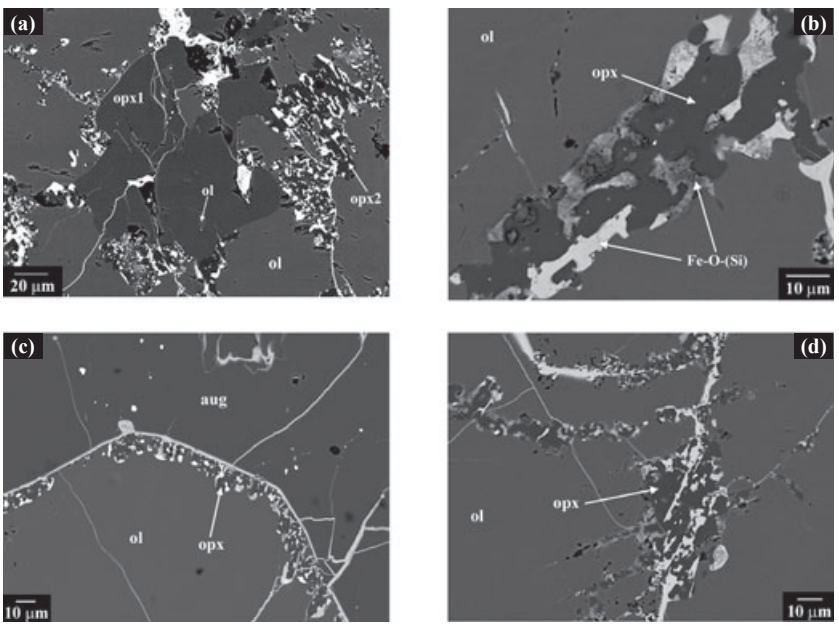

Fig. 4. Backscattered electron images of fine-grained assemblages of orthopyroxene + opaque phases in NWA 1500 and possibly related meteorites studied here. a) NWA 1500, showing two types of orthopyroxene. Opx 1 (containing islands of olivine) is inferred to have formed by the olivine + melt → orthopyroxene reaction. Opx 2 is in grain-broundary assemblages intergrown with opaque phases. b) Reid 013. c) NWA 595. d) Hughes 026. Note strong alignment and euhedral/subhedral shapes of opaques in (b) and (d).

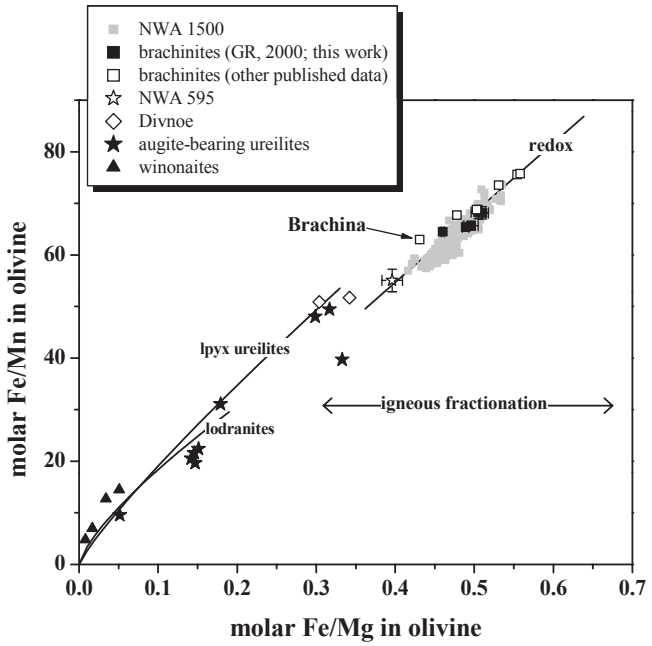

Fig. 5. Molar Fe/Mg ratio versus molar Fe/Mn ratio in olivine in various primitive achondrites. Trend of the olivine-pigeonite and olivine-orthopyroxene ureilites (lpyx ureilites) is defined by a self-consistent set of high precision analyses, and is nearly a pure redox trend (Goodrich et al. 1987, 2006; Goodrich and Righter, 2000); data points defining the trend are not shown. All augite-bearing ureilites plot to the right of this trend within the same range of Fe/Mg ratios. Acapulcoites/lodranites and winonaites show redox trends similar to that of olivine-lpyx ureilites. Olivine in brachinites has higher Fe/Mg ratio than in any other group and forms a short redox trend of lower slope (higher Mn/Mg ratio). Olivine in NWA 1500 shows a well-defined redox trend, nearly coincident with the brachinite data. However, note that the brachinite trend is formed by different samples (each of which is homogeneous), while the NWA 1500 trend is internal (reflecting reverse zonation of olivine grains). Sources of data as follows. NWA 1500: Goodrich et al. (2006). Ureilites: Goodrich et al. (1987, 2001, 2006); Goodrich and Righter (2000). Brachinites: This work (Table 5); Goodrich and Righter (2000); Mittlefehldt et al. (2003); Warren and Kallemeyn (1989). Winonaites/IAB: Benedix et al. (1998); Kimura et al. (1992). Acapulcoites and lodranites: Unpublished data of the first author for nine lodranites; Papike et al. (1995); Nagahara (1992); Mittlefehldt et al. (1996); Burroni and Folco (2008); Takeda et al. (1994). Divnoe: Petaev et al. (1994). NWA 595: This work (Table 5).

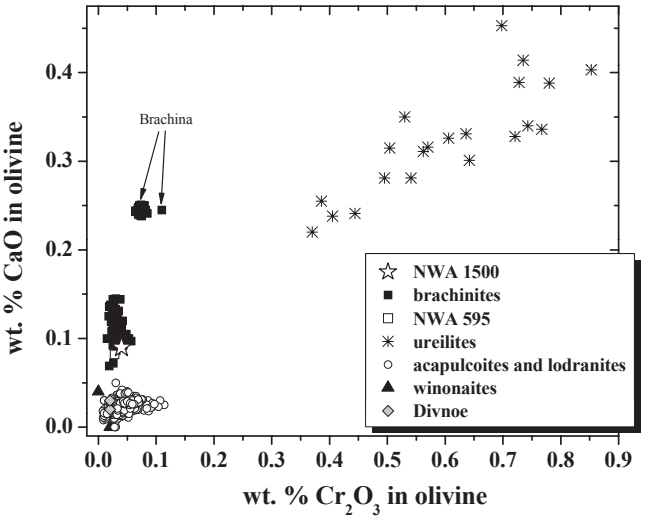

Fig. 6. CaO and Cr_2O_3 contents of olivine in various primitive achondrites. Sources of data as in Fig. 5.

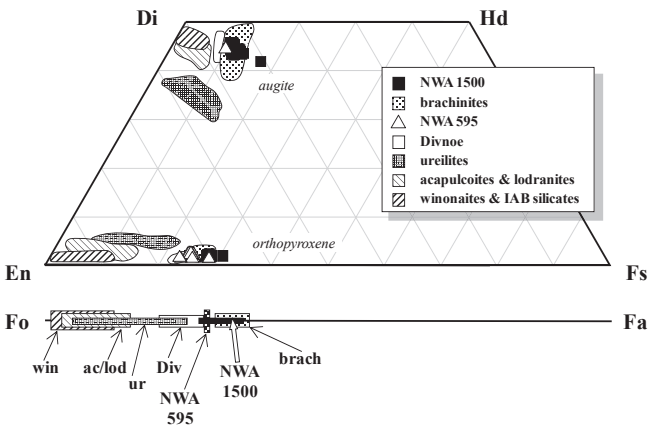

Fig. 7. Pyroxene quadrilateral showing compositions of augite and orthopyroxene in various primitive achondrites. Compositions of olivine (Fo-Fa) in the same groups shown at bottom. Orthopyroxene in brachinites is from grain boundary assemblages. Orthopyroxene in NWA 595 includes both coarse orthopyroxene and grain boundary orthopyroxene. Sources of data as follows. NWA 1500: Goodrich et al. (2006); Brachinites: Johnson et al. (1977); Nehru et al. (1983); Warren and Kallemeyn (1989); Grossman (1998); Goodrich and Righter (2000); Mittlefehldt et al. (2003); Connolly et al. (2006, 2008); This work (Table 6). NWA 595: This work (Table 6). Divnoe: Petaev et al. (1994). Winonaites/IAB: Benedix et al. (1998); Kimura et al. (1992). Lodranites and acapulcoites: Takeda et al. (1994); McCoy et al. (1996); Burroni and Folco (2008); Mittlefehldt et al. (1996); Nagahara (1992). Ureilites: Takeda (1987, 1989); Takeda et al. (1989); Weber et al. (2003); Goodrich et al. (2001, 2009); unpublished data of the first author (LEW 88774).

Wo < 1, *mg* 76–77. The large poikilitic plagioclase grains are An_{37-39}; the small interstitial grains are An_{32-33} (Fig. 9).

Comparison of NWA 1500 to Brachinites and Other Olivine-Rich Primitive Achondrites

Fourteen meteorites (after pairings) are currently recognized as brachinites (Table 4), but 10 of these have previously been described only in abstracts or the Meteoritical Bulletin. We report new data for three of the latter (Reid 013, Hughes 026, and NWA 5191).

Brachinites are olivine-rich (79–95%) achondrites characterized by relatively FeO-rich mineral compositions (Fo 64–70) and significant abundances of augite. They have diverse plagioclase contents, ranging from approximately 10% in the type specimen Brachina to none in other samples (Table 4; Fig. 2). Minor orthopyroxene, chromite, phosphates, sulfide, and metal have been reported in most brachinites. NWA 595 was initially classified as a brachinite (Connolly et al. 2006). However, Irving et al. (2005) pointed out that it contains significantly more orthopyroxene than most brachinites and suggested that it be reclassified as ungrouped. We report new observations and data for this meteorite. Divnoe was originally thought to be a brachinite because of its oxygen isotope composition (Fig. 1), but was subsequently recognized as petrologically and chemically unique (Petaev et al. 1994). The sodic plagioclase-dominated achondrite GRA 06128/06129 has an oxygen isotope composition within the range of brachinites (Fig. 1) and has been suggested to be related to them (Ziegler et al. 2008; Day et al. 2009; Shearer et al. 2010). However, because GRA 06128/06129 is not an olivine-rich meteorite, it is not within the scope of this comparison.

Textures

The olivine-rich areas of most brachinites have protogranular textures, with rounded grain boundaries and common triple junctions (although a variety of other terms have also been used to describe this texture). Typical grain sizes are in the range 0.1–1.5 mm, averaging approximately 0.6–0.7 mm (Table 4). Augite grains are generally larger (up to 1–2 mm) and show intergranular forms. The distribution of both augite and plagioclase is commonly heterogeneous. Brachina is exceptional in being finer-grained (0.1–0.3 mm) and having a wholly equigranular texture (Johnson et al. 1977; Nehru et al. 1996). Nevertheless, reports for most brachinites indicate significant internal variation in texture from equigranular to more prismatic olivine shapes (e.g., Warren and Kallemeyn 1989; Mittlefehldt et al. 2003). Weak preferred orientation and foliation have been reported in Allan Hills (ALH) 84025 and Elephant Moraine (EET) 99402/7 (Warren and Kallemeyn 1989; Mittlefehldt et al. 2003). Two recently described brachinites, NWA 4872 and NWA 4969 have a bimodal distribution of olivine sizes, with large (0.3–1.1 mm) grains set in a matrix of fine (0.02–0.3 mm) grains (Rumble et al. 2008).

Of the samples studied here, NWA 5191 and Hughes 026 have protogranular textures similar to those of most brachinites (Fig. 3b). This is true for most of Reid 013 as well, but two of the three sections we studied also contain vein-like areas (~0.5 mm wide and extending across the whole section) with much smaller (~0.02 mm) grain size (Fig. 3c). NWA 595 has a more complex texture. As noted in the original description (Connolly et al. 2006), olivine-rich areas have a protogranular (polygonal-granular) texture similar to most brachinites, with alignment of elongated grains. However, we have found that its pyroxenes are coarsely poikilitic, with both augite and orthopyroxene enclosing rounded grains of olivine and each enclosing rounded grains of the other (Fig. 3d).

The textures of brachinites (with the possible exception of Brachina) are distinguished from those of most acapulcoites and winonaites in being coarser-grained and less-equilibrated, and they lack the complexities (e.g., several distinct lithologies) of Divnoe (Petaev et al. 1994). However, they are not clearly distinguished from the textures of many lodranites or ureilites (Mittlefehldt et al. 1998). The texture of NWA 1500 is similar to that of most brachinites, but it should be noted that its textural resemblance to ureilites was one of the reasons why it was originally thought to be a ureilite (Bartoschewitz et al. 2003; Goodrich et al. 2006). The vein-like areas of NWA 1500 are similar to the veins in Reid 013 in having a concentration of plagioclase and fine-grained orthopyroxene, but the large grain size and poikilitic texture of the plagioclase are features not observed in brachinites.

Modal Abundances

Modal abundances determined in this work for Reid 013, Hughes 026, and NWA 5191 are within the range of those in other brachinites (Table 4). However, the vein-like areas of Reid 013 have significant concentrations of augite, plagioclase, and orthopyroxene relative to the bulk (e.g., 6% plagioclase versus only a trace). Modal abundances determined in this work for NWA 595 show less pyroxene (3% versus 5–10% augite and 6.5% versus 10–15% orthopyroxene) than initially reported (Connolly et al. 2006), but a similar orthopyroxene/augite ratio (Table 4; Fig. 2a).

Brachinites are clearly distinguished from the other major groups of primitive achondrites by modal abundances of major silicate minerals (Fig. 2a). Their high augite/orthopyroxene ratios distinguish them from Divnoe, NWA 595, acapulcoites, lodranites, and winonaites/IAB silicates, whereas the presence of plagioclase (at least as a group feature) distinguishes them from augite-bearing ureilites. They are also distinguished from acapulcoites, lodranites, and winonaites/IAB silicates by low metal contents (Fig. 2b), and from acapulcoites and winonaites by lower sulfide contents (Fig. 2c). Modal abundances of silicates, metal, sulfide, and other minor phases in NWA

1500 are all within the range of those in brachinites (Table 4), and thus distinguished from those of the other groups (Fig. 2).

Grain Boundary Assemblages of Orthopyroxene + Opaques

Fine-grained assemblages of orthopyroxene plus opaque minerals are pervasive in Reid 013, Hughes 026, NWA 5191, and NWA 595. They occur along all olivine-olivine, olivine-augite, and olivine-chromite grain boundaries, as veins extending into olivine, and surrounding inclusions within olivine (Figs. 3b and 4). Rumble et al. (2008) also reported these assemblages in NWA 4882, NWA 4874, NWA 4969, and NWA 4872, but their existence is not mentioned in published descriptions of any other brachinites. We searched for them in Brachina and found that they are absent. Within these assemblages, the opaques commonly show elongated, subhedral shapes, and preferred alignment (Figs. 4b and 4d). Most of them are Fe-oxides, with highly variable Fe, O, Si, Mg, and S contents (and low electron microprobe analysis [EMPA] totals). Textures and compositions suggest that they are alteration products (most likely due to terrestrial weathering) of metal and/or sulfide. Preserved sulfides are not uncommon within these assemblages, but metal is very rare. Grains of augite and rare chromite are also observed. Rumble et al. (2008) reported fayalite in these assemblages, but our observations do not confirm this. Although some of the Fe-oxide grains we analyzed had high SiO_2 contents approaching that of fayalite (~30 wt%), none were consistent with fayalite stoichiometry.

The orthopyroxene + opaques assemblages that occur along grain boundaries and within olivine in NWA 1500 are virtually identical to these assemblages in Reid 013, Hughes 026, NWA 5191, and NWA 595. To our knowledge, such assemblages do not occur in any other primitive achondrites (e.g., Mittlefehldt et al. 1998).

Mineral Compositions

Olivine in brachinites is more ferroan (Fo 64–70) than in any other group of primitive achondrites, and is distinguished by other compositional parameters as well (Figs. 5–7). Fe/Mg-Fe/Mn compositions of olivine are particularly useful for identifying meteorite groups and interpreting petrogenesis (Fig. 5). Our new data for NWA 5191 and NWA 595 (Table 4) augment an existing self-consistent set of high precision data for Fe-Mn-Mg compositions of olivine in 23 ureilites, 9 lodranites, and the 4 brachinites—Brachina, Reid 013, Hughes 026, and ALH 84025 (Goodrich et al. 1987, 2001, 2006; Goodrich 1998; Goodrich and Righter 2000). This data set shows that the olivine + low-Ca pyroxene (lpyx) ureilites define a characteristic Fe/Mg-Fe/Mn trend consistent with a nearly pure redox relationship (Fig. 5). Lodranites define a similar trend, and literature data for winonaites suggest that they do as well (Fig. 5). Brachinites occupy a distinct region of Fe-Mn-Mg space (Fig. 5), and form a short redox trend at higher Mn/Mg ratio than the olivine-lpyx ureilite, lodranite, and winonaite trends. Olivine in NWA 595 is consistent with this trend and extends it to lower Fe/Mg ratio. Olivine in Divnoe, however, plots closer to the olivine-lpyx ureilite trend (Fig. 5). Relative to the olivine-lpyx ureilites, the augite-bearing ureilites all have higher Mn/Mg ratios similar to those of brachinites, but are well distinguished from brachinites by being more magnesian (Fig. 5).

Table 5. Compositions of olivine in NWA 5191 and NWA 595.

	NWA 595		NWA 5191	
	Average (22)[a]	SD (22)	Average (22)[a]	SD (22)
SiO_2	37.4	0.1	36.8	0.1
Cr_2O_3	0.028	0.008	0.035	0.015
FeO	25.7	0.5	30.0	0.3
MgO	36.5	0.4	33.3	0.3
MnO	0.462	0.012	0.434	0.009
CaO	0.082	0.012	0.131	0.022
Total	100.2	0.3	100.8	0.2
Fo	71.7	0.63	66.4	0.41
Fe/Mg	0.396	0.013	0.505	0.009
Fe/Mn	55.1	2.2	68.3	1.3

Note: Fo = mole percent forsterite; Fe/Mg = molar Fe/Mg; Fe/Mn = molar Fe/Mn.
[a]Analytical precision (2σ) is reflected in significant digits.

Olivine in brachinites is also distinguished by having lower Cr_2O_3 and (with the exception of Brachina) CaO contents than olivine in ureilites, and higher CaO than olivine in acapulcoites, lodranites, winonaites/IAB silicates, and Divnoe (Fig. 6). Olivine in NWA 595 has CaO and Cr_2O_3 contents within the range of brachinites (Table 5; Fig. 6).

In terms of all these aspects of olivine composition, NWA 1500 is within the range of brachinites, and thus distinguished from other primitive achondrites (Figs. 5–7). In particular, the well-defined Fe/Mg-Fe/Mn redox trend shown by NWA 1500 is nearly coincident with the more diffuse brachinite trend (Fig. 5). A significant difference, however, is that the NWA 1500 trend is internal to the meteorite (reflecting the reverse zonation of olivine cores and reduction rims), whereas the brachinite trend exists only among the different samples (i.e., olivines within each brachinite are homogeneous).

Augite in brachinites, including new data for NWA 5191 (Table 6), is more ferroan (*mg* 77–82) than that in any other primitive achondrites except the most ferroan ureilites, and is distinguished from the latter by

Table 6. Compositions of pyroxenes and plagioclase in Hughes 026, Reid 013, NWA 3151, and NWA 595.

	Augite				Orthopyroxene			Plagioclase		
	Hughes 026 (8)	Reid 013 (6)	NWA 5191 (84)	NWA 595 (14)	NWA 5191 gb (17)[a]	NWA 595 coarse (25)	NWA 595 gb (5)[a]	Hughes 026 (3)	Reid 013 (5)	Reid 013 (5)[b]
SiO_2	53.6	53.5	53.8	53.4	54.2	54.4	54.0	58.8	59.7	60.1
TiO_2	0.14	0.12	0.09	0.14	0.02	0.07	0.02	bdl	bdl	bdl
Al_2O_3	1.01	0.74	0.99	0.78	0.11	0.40	0.04	25.4	24.5	24.3
Cr_2O3	0.76	0.61	0.75	0.62	0.13	0.22	0.07	0.03	0.02	0.02
FeO	6.19	7.09	6.1	6.1	17.9	16.2	17.1	0.19	0.11	1.12
MgO	15.2	15.7	15.3	16.1	26.1	26.7	27.3	0.02	0.02	0.03
MnO	0.16	0.18	0.15	0.20	0.4	0.40	0.44	0.03	0.01	0.02
CaO	22.6	22.0	22.7	21.6	1.41	1.10	0.75	7.75	6.82	6.40
K_2O	bdl	bdl	na	na	na	na	na	0.05	0.10	0.11
Na_2O	0.42	0.37	0.47	0.36	0.02	0.03	0.01	7.08	7.52	7.76
Total	100.0	100.3	100.3	99.3	100.3	99.5	99.8	99.4	98.8	99.8
Mole percent										
Fs	9.9	11.2	9.7	9.8	27.1	24.8	25.7			
Wo	46.5	44.6	46.7	44.4	2.7	2.2	1.4			
En	43.5	44.1	43.7	45.9	70.2	73.0	72.9			
An								37.6	33.2	31.1
Or								0.3	0.6	0.7
Ab								62.1	66.3	68.2

Note: bdl = below detection limit; na = not analyzed; Fs = ferrosilite; Wo = wollastonite; En = enstatite; An = anorthite; Or = orthoclase; Ab = albite.

[a]In grain boundary orthopyroxene + metal assemblages.

[b]In finer-grained veins.

significantly higher Wo (Fig. 7). In addition, it has distinctly lower Al_2O_3 and Cr_2O_3 contents, and higher TiO_2 content, than ureilitic augites of similar *mg* (Fig. 8). Augite in NWA 595 is similar to that in the more magnesian brachinites (*mg* 82.4; Table 6), although with slightly lower Al_2O_3 and Cr_2O_3 and higher TiO_2 (Fig. 8). Augite in Divnoe has significantly higher *mg* and lower Al_2O_3, Cr_2O_3, and TiO_2 contents than that in brachinites (Figs. 7 and 8). Orthopyroxene in the grain boundary assemblages in brachinites is more ferroan (*mg* 71–74) than that in any other primitive achondrites (Fig. 7; Table 6). This is also true of both the coarse and the grain boundary orthopyroxene in NWA 595 (Fig. 7; Table 6). In terms of all aspects of pyroxene composition, NWA 1500 is within the range of brachinites and distinguished from other groups (Figs. 7 and 8).

Compositions of plagioclase in brachinites encompass a higher range of An contents ($\sim An_{22-40}$) than those in other groups of olivine-rich primitive achondrites, although they overlap with observed ranges of all groups (Fig. 9). The composition of plagioclase in Divnoe is within the brachinite range. Plagioclase in NWA 1500 (An_{32-39}) has a compositional range very similar to that of brachinites, with higher An content than any other groups except lodranites (Fig. 9).

Geochemistry

Certain aspects of bulk composition can be useful for distinguishing groups of meteorites and revealing differences in petrogenesis, with the caveats that analyses of bulk samples can be affected by unrepresentative sampling of heterogeneously distributed phases, and that some trace elements (e.g., light rare earth elements [LREE], K) are easily disturbed by terrestrial weathering. Figure 10 shows CI-normalized REE abundances in brachinites, including new data from this work for Hughes 026 and Reid 013 (Table 7). Brachina has nearly chondritic abundances of all REE. In contrast, ALH 84025, EET 99402/7, and one sample of Reid 013 (Reid 013-1; Table 7) have subchondritic abundances and LREE-depleted patterns with CI-normalized Sm/Eu = 0.19–0.35. Eagle's Nest has much higher REE abundances and a strongly LREE-enriched pattern, which (along with extremely high K abundance) are likely due to terrestrial contamination (Swindle et al. 1998). Our sample of Hughes 026 and second sample of Reid 013 (Reid 013-2; Table 7) are also strongly LREE-enriched. However, Hughes 026 does not have high K (compared, for example, to Eagle's Nest) and its LREE-enrichment could also be due to a relative overabundance of apatite (e.g., Wadhwa et al. 1998a). Reid 013-2 has slightly elevated K ($\sim 5\times$ higher than Reid 013-1 and

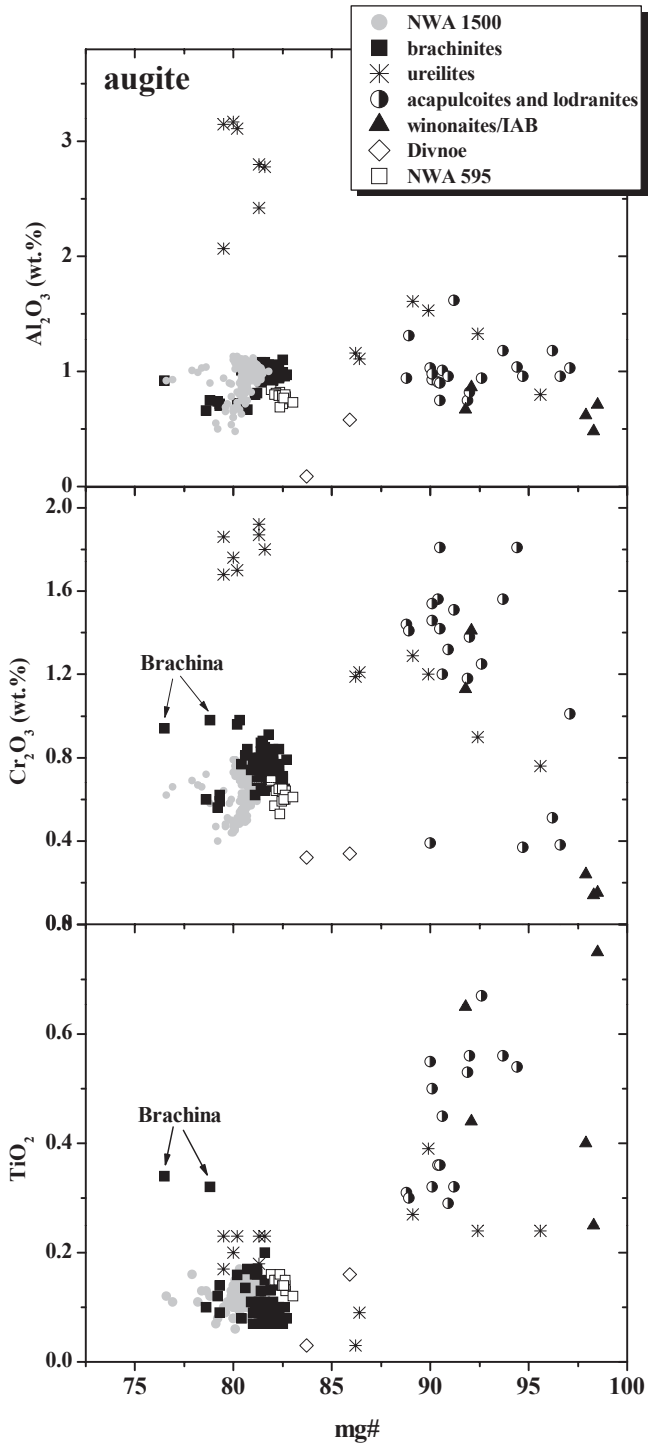

Fig. 8. Minor elements in augite in various primitive achondrites. Sources of data as in Fig. 7.

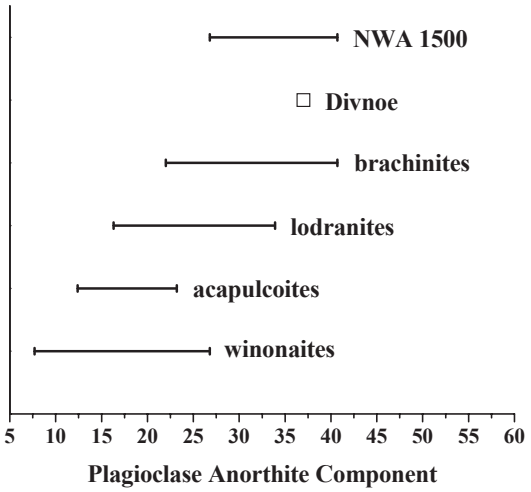

Fig. 9. Compositional ranges of plagioclase in various primitive achondrites. Sources of data as follows. Brachinites: as in Fig. 2. Acapulcoites: Mittlefehldt et al. (1996); Mittlefehldt et al. (1998) and references therein; Burroni and Folco (2008). Lodranites: Takeda et al. (1994), Nagahara and Ozawa (1986); Nagahara (1992); McCoy et al. (1997); Mittlefehldt et al. (1998) and references therein. Winonaites/IAB: Benedix et al. (1998); Kimura et al. (1992).

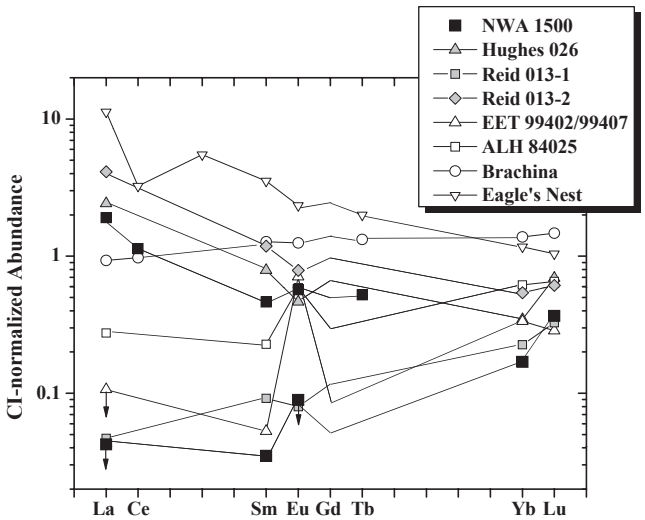

Fig. 10. CI-normalized rare earth element (REE) abundances in bulk samples of brachinites and NWA 1500. Sources of data as follows. NWA 1500: Goodrich et al. (2006). Brachinites: Swindle et al. (1998); Mittlefehldt et al. (2003); Nehru et al. (1983); Warren and Kallemeyn (1989); This work (Table 7). Values for Sm and Eu for NWA 1500 sample 2 given in Table 5 of Goodrich et al. (2006) are incorrect. Correct values are Sm = 0.069 ppm and Eu = 0.032 ppm.

$\sim$2.5 $\times$ higher than Hughes 026), which suggests some degree of contamination. Of two samples of NWA 1500 analyzed by Goodrich et al. (2006), one (NWA2) has a LREE-enriched pattern and extremely high K abundance that probably result from contamination; the other (NWA1) has a strongly LREE-depleted pattern very similar to those of the depleted brachinites such as Reid 013-1 (Fig. 10).

Table 7. Bulk compositions of brachinites Hughes 026 and Reid 013 from INAA[a].

	Hughes 026		Reid 013-1		Reid 013-2		Reid 013
Weight (mg)	174.13	SD (%)	188.02	SD (%)	174.13	SD (%)	Average
Al%	0.13	4	0.12	15	0.32	4	0.22
Mg%	17.8	3	16.7	3	16.6	3	16.65
Ti%	0.07	u.l.	0.1	u.l.	0.09	u.l.	
Ca%	0.57	12	0.5	20	0.72	12	0.61
V	84.8	4	72.4	4	83.5	4	77.95
Na	238	3	279	3	1113	3	696
K	54	7	26	10	126	5	76
Sc	6.74	3	6.41	3	6.86	3	6.64
Cr	4870	3	4300	3	4720	3	4511
Mn	2940	3	2790	3	2950	3	2870
Fe%	23.12	3	23.32	3	24.66	3	23.99
Co	165	3	284	3	273	3	278.5
Ni	3400	7	2530	4	2565	3	2548
Cu	15	u.l.	18	25	70	u.l.	
Zn	156	5	40.5	7	45	10	42.25
Ga	2.5	7	1.9	7	2.72	7	2.31
As	0.13	7	0.18	10	0.458	7	0.319
Se	0.8	u.l.	4.2	7	3.53	10	3.865
Br	0.37	7	1.12	4	0.877	4	0.9985
Sb	0.018	30	0.01	u.l.	0.032	25	0.032
Cs	0.15	u.l.	0.17	u.l.	0.6	u.l.	
Ba	15	u.l.	10	u.l.	25	u.l.	
La	0.572	4	0.011	25	0.972	25	0.4915
Sm	0.118	3	0.0137	7	0.176	7	0.09485
Eu	0.026	10	0.0045	15	0.044	15	0.02425
Ho	0.036	25			0.038	15	0.038
Yb	0.055	10	0.036	25	0.086	15	0.061
Lu	0.017	25	0.008	25	0.015	15	0.0115
Hf	0.13	u.l.	0.09	u.l.	0.19	u.l.	
Ta	0.09	u.l.	0.07	u.l.	0.113	u.l.	
W	0.1	u.l.	0.053	30	0.09	u.l.	
Re			0.056	15	0.015	u.l.	0.056
Os			0.21	15	0.22	15	0.215
Ir	0.011	15	0.0868	4	0.1	7	0.0934
Pt	1.6	u.l.	1.5	u.l.	0.37	u.l.	
Au	0.0194	4	0.0184	3	0.014	3	0.0162
Hg			0.15	u.l.	0.5	u.l.	
Th	0.16	u.l.	0.08	u.l.	0.124	u.l.	
U	0.015	u.l.	0.03	u.l.	0.03	u.l.	

Note: u.l. = upper limit.
[a]Values in ppm unless otherwise specified.

A plot of CI-normalized Sm/Sc versus Na/Sc ratio (Fig. 11) can be used as a general indicator of degree of silicate melt extraction. Since Na and Sm are incompatible lithophile elements and Sc is a moderately compatible lithophile element, Sm/Sc/CI and Na/Sc/CI should both decrease (to roughly the same degree) with progressive depletion of a low-degree melt component (i.e., coupled loss of plagioclase and pyroxene). On this plot, acapulcoites and winonaites show near-chondritic compositions, whereas lodranites are clearly depleted, and ureilites even more so. Brachinites show a large range, with Brachina being nearly chondritic (similar to acapulcoites), and ALH 84025 and Reid 013-1 being as depleted as many ureilites. NWA 1500 (NWA1) shows an even higher degree of depletion than ureilites. Effects of unrepresentative sampling and contamination can also be seen on this plot. Eagle's Nest, NWA2, and Reid 013-2 all show enrichment in Sm/Sc relative to their Na/Sc ratios, which is indicative of contamination. This is true for Hughes 026 as well, although as suggested above this may be due to an excess of apatite rather than contamination. The higher Na/Sc ratio of

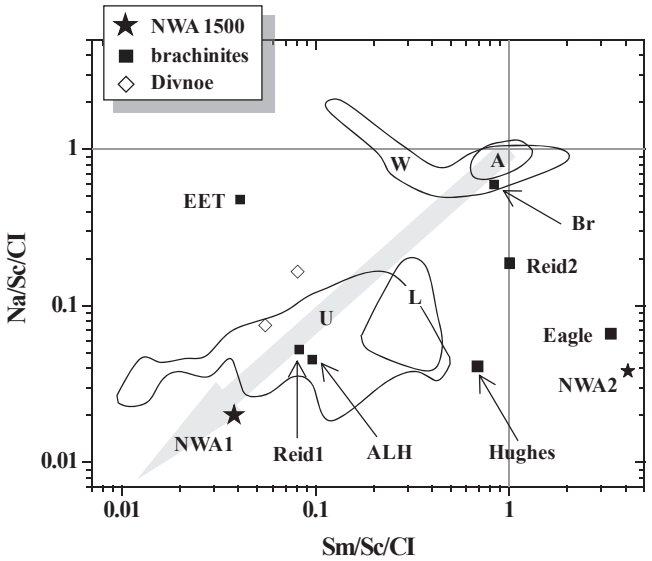

Fig. 11. CI-normalized Sm/Sc versus Na/Sc for bulk samples of various primitive achondrites. Light gray arrow shows a general trend for increasing degrees of silicate melt extraction (coupled loss of plagioclase and pyroxene). Fields for acapulcoites (A), lodranites (L), winonaites and IAB silicate inclusions (W) and ureilites (U) are representative of observed range for most data (not necessarily exhaustive). B = Brachina. ALH = ALH 84025. Reid1 and Reid2 = Reid 013-1 and Reid 013-2. Hughes = Hughes 026. EET = average of EET 99402 and EET 99407. NWA1 and NWA2 = NWA 1500 samples 1 and 2. Eagle = Eagle's Nest. Sources of data as follows. NWA 1500: Goodrich et al. (2006). Brachinites: Johnson et al. (1977); Nehru et al. (1983); Warren and Kallemeyn (1989); Mittlefehldt et al. (2003); This work (Table 7). Ureilites: Warren and Kallemeyn (1992); Warren et al. (2006). Winonaites and IAB silicates: Mittlefehldt et al. (1998) and references therein; Kimura et al. (1992). Acapulcoites and lodranites: Mittlefehldt et al. (1998) and references therein; Patzer et al. (2004). ALH 84302, a transitional member of the acapulcoite/lodranite group, is not plotted.

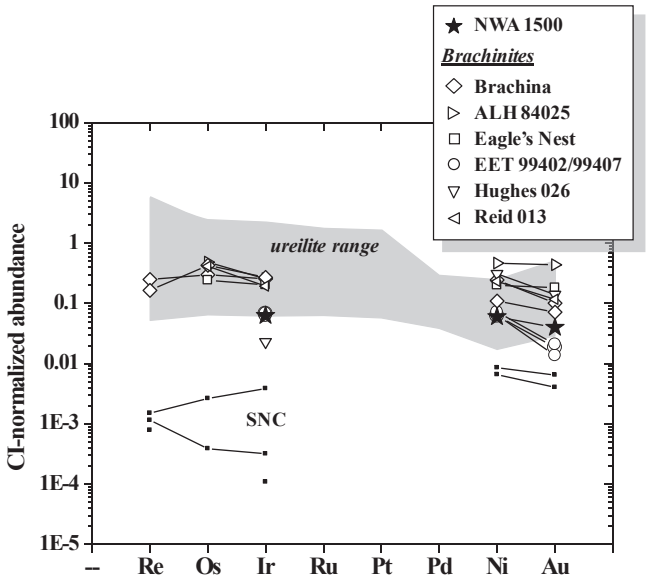

Fig. 12. CI-normalized abundances of siderophile elements in NWA 1500, brachinites, main group ureilites and Martian (SNC) meteorites. Sources of data as follows. NWA 1500: Goodrich et al. (2006). Brachinites: Nehru et al. (1983); Johnson et al. (1977); Dreibus et al. (1982); Swindle et al. (1998); Mittlefehldt et al. (2003); Warren and Kallemeyn (1989); This work (Table 7). Ureilites: Rankenburg et al. (2008); Warren and Kallemeyn (1992); Warren et al. (2006); Janssens et al. (1987); Kallemeyn and Warren (1994); SNC (Chassigny, Nakhla, and Lafayette): Treiman et al. (1986).

Reid 013-2 compared to Reid 013-1 is probably due to an excess of plagioclase, since this sample also has higher abundances of Ca and Al that are unlikely to be due to contamination.

Primitive achondrites tend to have high (near-chondritic) abundances of siderophile elements compared to rocks from highly differentiated bodies such as Mars, Moon, and Earth. Ureilites are a well-documented example of this, with siderophile element abundances in the range of approximately 0.1–5 × CI, 2–3 orders of magnitude higher than in SNC (Martian) meteorites (Fig. 12). Brachinites have siderophile element abundances that are within the range of ureilites, and NWA 1500 is clearly very similar to brachinites (Fig. 12). Moreover, the brachinite pattern, as gauged by Ir/Ni and Ni/Au ratios, is distinguished from that of ureilites, and NWA 1500 shares this pattern. As illustrated in Fig. 13,

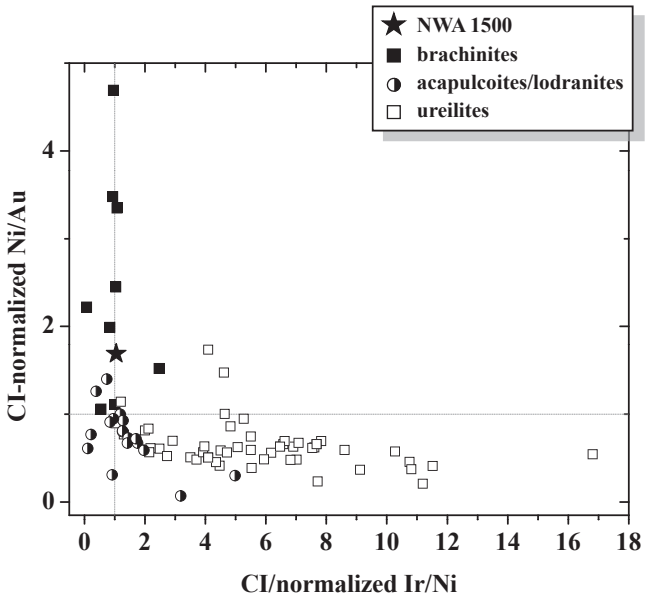

Fig. 13. CI-normalized Ni/Au and Ir/Ni in NWA 1500, brachinites, acapulcoites/lodranites, and ureilites. Sources of data as follows. NWA 1500, brachinites, and ureilites: as in Fig. 12. Acapulcoites and lodranites: Mittlefehldt et al. (1998) and references therein; Patzer et al. (2004).

ureilites have superchondritic Ir/Ni and near-chondritic to subchondritic Ni/Au ratios, whereas brachinites have near-chondritic Ir/Ni and superchondritic Ni/Au (acapulcoites and lodranites form an intermediate group, with near-chondritic values of both ratios). NWA 1500 plots within the range of brachinites on this diagram.

DISCUSSION

Is NWA 1500 a Brachinite?

Our new data show that bulk and individual mineral oxygen isotope compositions of NWA 1500 (Fig. 1) are similar to those of brachinites, Divnoe, NWA 595 and GRA 06128/06129, and distinguished from those of the other major groups of olivine-rich primitive achondrites (winonaites/IAB silicates, acapulcoites/lodranites, and ureilites). These data thus confirm the bulk oxygen isotope composition reported by Greenwood et al. (2007), rather than the original composition reported for this meteorite (Bartoschewitz et al. 2003). In addition, we find that modal mineral abundances, texture, olivine and pyroxene major and minor element compositions, plagioclase major element compositions, REE abundances, and siderophile element abundances of NWA 1500 are all within the range of those in brachinites and, in most cases, well distinguished from those of winonaites/IAB silicates, acapulcoites/lodranites, ureilites, Divnoe, and NWA 595. Thus, it is reasonable to consider whether NWA 1500 should be classified as a brachinite. The current classification scheme for meteorites (Weisberg et al. 2006) is largely based on their mineralogical and petrographic characteristics, combined with bulk geochemical and oxygen isotope compositions. By these criteria, NWA 1500 could clearly be classified as a brachinite, which leads one to ask why it was originally thought to be a ureilite (despite an apparently anomalous oxygen isotope composition) and the possibility of it being a brachinite not even considered (Bartoschewitz et al. 2003; Goodrich et al. 2006). The answer to this question draws attention to the most significant difference between NWA 1500 and brachinites. NWA 1500 has a compelling resemblance to ureilites in transmitted light (see Fig. 2a of Goodrich et al. 2006), due to grain boundary darkening that results from the "reduction rims" on olivine. As reduction rims on olivine are both a characteristic, and an apparently unique, feature of ureilites (Mittlefehldt et al. 1998), it is not surprising that the similarity of NWA 1500 to brachinites was overlooked. Indeed, our new observations confirm the lack of reverse zonation (or any zonation at all) of olivine in brachinites. However, we found that grain boundary assemblages of orthopyroxene + opaques, which may also be a product of late reduction in NWA 1500, occur in several brachinites. In the following section, we discuss the origin of these assemblages and implications for a NWA 1500-brachinite connection.

Reverse Zonation of Olivine and Grain Boundary Assemblages of Orthopyroxene + Opaques

Goodrich et al. (2006) distinguished between gently reverse-zoned but generally metal-free cores, and more steeply reverse-zoned, metal-bearing rims of olivine grains in NWA 1500, identifying the latter as "reduction rims" similar to those found in ureilites. However, our more detailed observations have shown that these rims contain far less metal than is typically found in reduction rims in ureilites (in some cases none at all), and so they should not necessarily be considered distinct from the cores. Furthermore, Goodrich et al. (2006) reported that the reduction rims in NWA 1500 sometimes consist of orthopyroxene rather than magnesian olivine. However, it now appears that this description is misleading. In fact, the grain boundary assemblages of orthopyroxene + opaques in NWA 1500 occur in addition to, rather instead of, the reversely zoned olivine rims (Fig. 3a). The grain boundary assemblages of orthopyroxene + opaques that we observed in Reid 013, NWA 5191, Hughes 026, and NWA 595, and that Rumble et al. (2008) observed in NWA 4882, NWA 4874, NWA 4969, and NWA 4872, are virtually identical to those in NWA 1500. The first step to understanding the origin of these assemblages is to establish the primary identity of their opaques. The textures and compositions of these opaques suggest that they are alteration products, most likely of metal and/or sulfide. As metal appears to weather more rapidly than sulfide in many meteorites (e.g., Wlotzka 1993a) and the S content of the opaques is usually low, it seems likely that the dominant original opaque in these intergrowths was metal. We have also considered the possibility that it was magnetite, but conclude that this is unlikely because magnetite should not be so highly susceptible to weathering (particularly when sulfide and some metal are preserved).

If we assume that these assemblages originally consisted of orthopyroxene + metal, we can consider three possibilities for their origin. These mechanisms are suggested by the observation that the assemblages are primarily associated with olivine (rather than any other primary mineral) and in many cases show textural evidence of having formed at the expense of olivine (Figs. 4c and 4d). (1) Rumble et al. (2008) suggested that these assemblages were similar to symplectic intergrowths of two pyroxenes + spinel ± metal that

occur as inclusions in olivine in a variety of rock types, and are products of late oxidation (Goodrich and Righter 2000). However, since we find that augite and chromite are only rare components of these assemblages (and we do not believe their primary opaques were magnetite), this origin seems unlikely. (2) A second possibility is that these assemblages formed by the normal peritectic reaction olivine + residual melt → orthopyroxene. However, in that case the presence of metal (as well as sulfide) in them would be purely fortuitous, which is inconsistent with the preferred alignment of metal grains within the orthopyroxene (Figs. 4b and 4d). Furthermore, at least in NWA 1500, it is clear that orthopyroxene formed by this normal fractionation reaction is compositionally and texturally distinct from the orthopyroxene in the grain boundary assemblages (Fig. 4a). (3) The third possibility for the origin of these assemblages, suggested by the preferred orientation of the metal grains in the orthopyroxene, is that they formed via the reduction reaction Mg_2SiO_4 + Fe_2SiO_4 = $2MgSiO_3$ + 2Fe + O_2, due to the presence of a reducing agent along grain boundaries (such as the graphite in ureilites). This interpretation is certainly plausible for NWA 1500, as the olivine shows evidence of reduction that increases in degree toward grain boundaries (i.e., reverse zoning) and the grain boundary orthopyroxene (opx2) is more magnesian than the presumably earlier-formed opx1 (*mg* 76–77 versus *mg* 71–72; Goodrich et al. 2006). However, it is less clear that this interpretation can be applied to NWA 595 and the brachinites. First of all, none of these samples show any zonation of olivine (although we cannot rule out the possibility that original reverse zonation has been eradicated by re-equilibration). Secondly, their grain boundary orthopyroxene is not obviously reduced. In NWA 595, it has *mg* identical to that of the primary (coarse-grained) orthopyroxene (Table 6). And in NWA 5191 and Reid 013, it is not significantly more magnesian than what would have been in equilibrium with coexisting olivine and augite at typical brachinite equilibration temperatures of approximately 850–950 °C (calculated using the program QUILF; Andersen et al. 1993). It is possible, of course, that these assemblages formed at lower temperatures and therefore their orthopyroxene actually is overly magnesian, but there is no direct evidence of this.

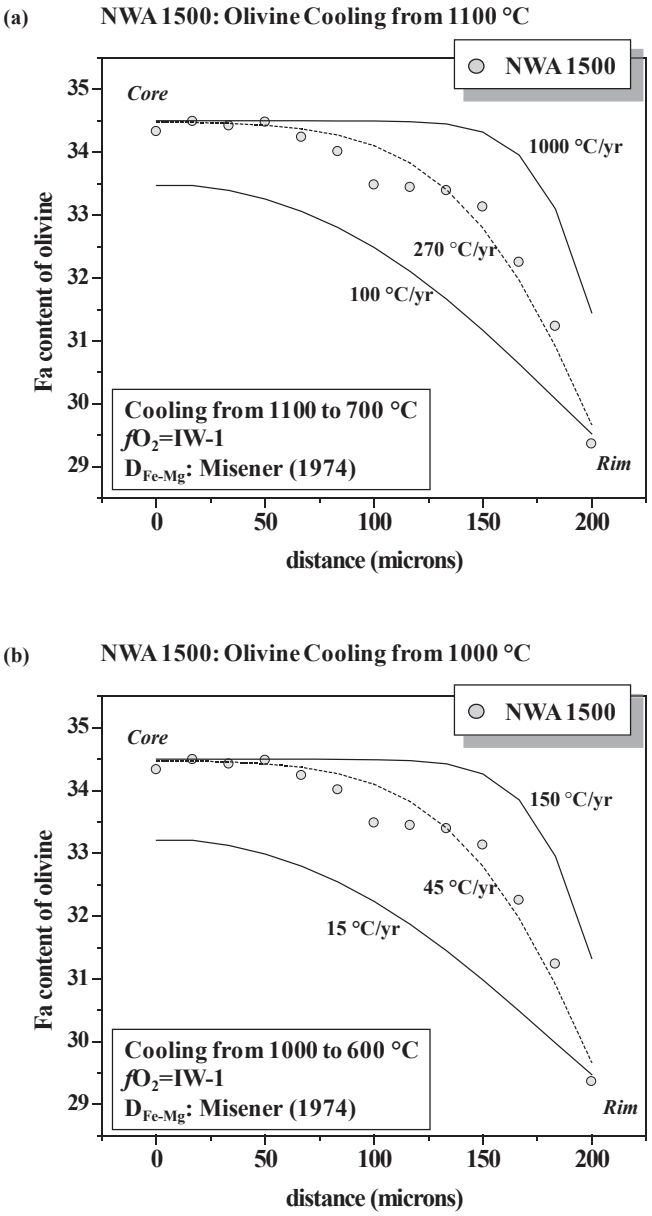

Fig. 14. Calculated Fe/Mg diffusion profiles for olivine, compared to the zonation profile of the most highly zoned olivine grain observed in NWA 1500 (Goodrich et al. 2006). Calculation is based on the assumption that zoning results from solid-state reduction of initially homogeneous olivine crystals by a reducing agent located along grain boundaries (see text for explanation).

At the same time, the presence of sulfide in these intergrowths (including those in NWA 1500) cannot be ignored (even if its abundance was originally less than that of metal). As sulfides clearly cannot be produced by reduction of olivine, their presence requires either an alternative or an additional explanation. Dispersion of tiny metal + sulfide grains within grain margins and along fractures or cleavage in silicates is observed in shocked ordinary chondrites and in many ureilites, and is attributed to shock heating and mobilization of liquid metal-sulfide (Rubin 2006). In ureilites, this phenomenon is sometimes observed in conjunction with reduction rims and veins, consistent with the interpretation that the late reduction is a consequence

of impact excavation (Mittlefehldt et al. 1998). This suggests the possibility that the observed assemblages of orthopyroxene + metal/sulfide formed in a shock event that led to both reduction of olivine and melting above the Fe-FeS eutectic temperature.

Nevertheless, the fact remains that (unlike ureilites) none of these rocks contain graphite, or evidence of any other reducing agent. Thus, we cannot even identify the specific mechanism that led to the reverse zonation of olivine in NWA 1500, say nothing of the grain boundary orthopyroxene + metal/sulfide assemblages in these samples. It is difficult to envision, however, that the reverse zonation is due to anything other than chemical reduction. Indeed, reverse-zoned olivines in a few pallasites and lodranites have been attributed to reduction without any identification of the reducing agent (e.g., Miyamoto and Takeda 1993; Mittlefehldt et al. 1998). In addition, some ureilites contain no carbon but nevertheless show typical reduction rims on their olivine (Goodrich et al. 2001). In these cases, it is generally assumed (by comparison to other ureilites, of course) that their original carbon was completely consumed by the reduction reaction. Thus, the absence of a reducing agent is not necessarily evidence against a reduction mechanism. In summary, it seems likely that the reversely zoned olivines in NWA 1500 are a product of reduction, in which case its orthopyroxene + metal/sulfide assemblages probably are too. Whether this is also the case for the orthopyroxene + metal/sulfide assemblages in NWA 595 and the brachinites is less clear, but reduction still appears to be the best hypothesis. Regardless of their origin, the existence of these assemblages reinforces the petrologic similarities between NWA 1500 and these other meteorites.

Comparison of Al-Mg Results to Age Data for Brachinites

The presence of large plagioclase grains in NWA 1500 is a valuable feature in that it offers the potential for high precision chronology using the ^{26}Al-^{26}Mg system. The results of our ^{26}Al-^{26}Mg analyses can be compared with available age data for brachinites, in particular the ^{53}Mn-^{53}Cr data of Wadhwa et al. (1998b) for Brachina. These data showed bulk rock, chromite, and silicate mineral fractions with resolvable ^{53}Cr excesses, well correlated with Mn/Cr ratio and defining a ^{53}Mn/^{55}Mn ratio of $(3.8 \pm 0.4) \times 10^{-6}$. This ratio corresponds to a relative age of 4564.5 ± 0.6 Ma (relative to the angrite Lewis Cliff 86010) or 4565.3 ± 0.6 Ma (relative to the angrite D'Orbigny), which is well within 5 Ma of CAI formation. In contrast, the lack of ^{26}Mg excess in NWA 1500 indicates that at the time of isotope closure ^{26}Al was already depleted at the level ^{26}Al/^{27}Al $\leq 10^{-7}$, corresponding to at least 7 Ma after CAI formation. This implies either a much younger formation age, or a more protracted cooling history, for NWA 1500 compared to Brachina. To evaluate these two alternatives, we next consider equilibration temperatures and cooling rates for NWA 1500 compared to those for brachinites.

Equilibration Temperatures and Cooling Rates

Our oxygen isotope data for olivine and plagioclase in NWA 1500 yield an equilibration temperature of 880 ± 70 °C, consistent with equilibration temperatures of 835–913 °C from two-pyroxene (augite plus the inferred primary orthopyroxene) thermometry and 877–1030 ± 40 °C from olivine-chromite thermometry (Goodrich et al. 2006). These temperatures are significantly lower than ureilite equilibration temperatures, which are in the range 1200–1300 °C (Mittlefehldt et al. 1998), and similar to the range of estimates for brachinites: 825–1070 °C from two-pyroxene (augite plus grain boundary orthopyroxene) and 800–1080 °C from olivine-chromite thermometry (Nehru et al. 1996). NWA 595 and NWA 5191 (Table 3) yield similar two-pyroxene (augite-orthopyroxene) equilibration temperatures: 928 ± 44 °C (using primary orthopyroxene) and 927 ± 67 °C (using grain boundary orthopyroxene), respectively (calculated using QUILF; Andersen et al. 1993). Brachina does not contain either primary or grain boundary orthopyroxene, but Nehru et al. (1983) calculated a two-pyroxene equilibration temperature in the range of 1000–1100 °C using orthopyroxene in melt inclusions. Although this temperature is somewhat higher than two-pyroxene temperatures for other brachinites and NWA 1500, it is not necessarily comparable because crystallization within melt inclusions may not be an equilibrium process. Furthermore, Brachina's olivine-chromite equilibration temperature is similar to that of other brachinites (Nehru et al. 1996). Thus, it appears that equilibration temperatures for NWA 1500 are similar to those for Brachina and other brachinites.

We calculated cooling rates from Fe/Mg zonation of olivine in NWA 1500, under the assumption that the zoning results from solid-state reduction of initially homogeneous olivine crystals by a reducing agent located along grain boundaries. We used a diffusion coefficient for Fe/Mg in olivine that was based on Misener (1974) and revised considering dependence on oxygen fugacity (Miyamoto et al. 2002). We assumed that fO_2 was buffered at 1 log unit below the iron-wüstite buffer; this is an oversimplification of the actual reduction reaction, but lowering fO_2 during the cooling is found to have little effect on our results. Diffusion

profiles were calculated for cooling over the temperature ranges of 1100–700 and 1000–600 °C. Cooling to lower temperatures leads to no significant difference in the results because atomic diffusion at low temperature is very slow and profile modification is mostly achieved at high temperature. Figure 14 shows the results of these calculations compared to the Fe/Mg zonation profile of the most highly zoned olivine grain observed by Goodrich et al. (2006). The best match to the observed zonation is a cooling rate of 270 °C yr^{-1} from 1100 to 700 °C, or 45 °C yr^{-1} from 1000 to 600 °C. These cooling rates are considerably lower than those calculated for ureilites ($1–5 \times 10^4$ °C yr^{-1}), but higher than those calculated for lodranites (2–3 °C yr^{-1}) using this method (Miyamoto et al. 1985, 1993; Miyamoto and Takeda 1994). The ureilite and lodranite calculations were based on the Fe/Mg diffusion rates of Buening and Buseck (1973), which give cooling rates roughly 1 order of magnitude higher than those from Misener (1974), but even if we consider this difference, the cooling rates obtained for NWA 1500 olivine are intermediate between those of ureilites and those of lodranites. Furthermore, they are several orders of magnitude faster than would be required for equilibration of anorthite, based on self-diffusion of Mg (LaTourrette and Wasserburg 1998), thus indicating that any ^{26}Mg excess present should have been preserved. In the simplest interpretation, this would imply that NWA 1500 is significantly younger than Brachina.

On the other hand, the calculated cooling rates are only relevant if it is correct that the zoning of olivine in NWA 1500 is due to solid-state reduction. Goodrich et al. (2006) suggested the alternative interpretation that the olivine grains are reverse-zoned because they crystallized under conditions of decreasing fO_2 due to ascent in a carbon-bearing magma, an interpretation that would be more consistent with the paucity of metal grains within the olivine. If this were the case, then it is still possible that original ^{26}Mg excesses were eradicated during slow cooling. Furthermore, it is possible that late shock heating, as in some brachinites (Mittlefehldt et al. 2003), erased any ^{26}Mg excesses, although the petrographic imprint of shock in NWA 1500 is not pronounced.

Finally, we note that even if NWA 1500 does have a younger crystallization age than Brachina, this conclusion cannot necessarily be extended to other brachinites. As discussed in the following section, it is not clear that all brachinites are derived from the same parent body, and Brachina itself shows a number of outlying features. Further evaluation of the implications of our ^{26}Al-^{26}Mg data for a comparison to brachinites will require ^{26}Al-^{26}Mg data for the latter, and/or application of other chronometers to NWA 1500.

Petrogenesis of Brachinites

Oxygen isotope data for brachinites show some variation in $\Delta^{17}O$, at the level of 0.1–0.2‰ (Fig. 1), with Brachina itself having one of the most extreme deviations from the majority of samples (Clayton and Mayeda 1996; Greenwood et al. 2007; Rumble et al. 2008). This variation may reflect a single parent body that was heated for insufficient time to erase accretional oxygen isotope heterogeneities (Rumble et al. 2008), or derivation from multiple parent bodies (Greenwood et al. 2007). The petrogenesis of brachinites is not well established, with the two main hypotheses being: (1) formation as residues of various degrees of partial melting and melt migration, analogous to the acapulcoite-lodranite clan (Nehru et al. 1983, 1996); or (2) formation as cumulates from a magma (Warren and Kallemeyn 1989; Swindle et al. 1998; Mittlefehldt et al. 2003). A residue model could be consistent with preservation of primary oxygen isotope heterogeneities (e.g., Goodrich et al. 2007; Wilson et al. 2008), whereas a cumulate model might require derivation from multiple parent bodies (see similar arguments for ureilites in Scott et al. 1993). In either model, however, Brachina seems to require special discussion (e.g., Mittlefehldt et al. 2003), and additional hypotheses that have been invoked to explain its origin include crystallization from a melt of its own composition (Johnson et al. 1977) or crystallization from an impact melt (Ryder 1982). Indeed, Brachina is distinguished from other brachinites, not only in oxygen isotope composition, but also in bulk chemical composition (which is closer to chondritic; Figs. 10–12), modal abundances (in particular, near-chondritic abundance of plagioclase), texture, the presence of melt inclusions in olivine (Nehru et al. 1983), and several mineral compositional parameters such as CaO and Fe-Mn-Mg in olivine and Cr_2O_3 and TiO_2 in augite (Figs. 5–7). Thus, there is considerable evidence that Brachina is not derived from the same parent body as other brachinites.

The possibility that brachinites are related to one another by various degrees of oxidation/reduction of common precursor material was first suggested by Fe-Mn-Mg data for olivine in four brachinites (Goodrich and Righter 2000). This observation was strengthened by new data from Mittlefehldt et al. (2003), and now appears well established from the expanded set of Fe-Mn-Mg data shown in Fig. 5. Such a relationship seems best explained by either multiple parent bodies (similar to the relationship among ordinary chondrite groups) or a single parent body and a residue origin (Goodrich and Delaney 2000), although Mittlefehldt et al. (2003) suggested that it could reflect differences in oxidation state among the source regions of different brachinite

parent magmas. If NWA 1500 is a brachinite, it may provide evidence that redox processes were important on a small (sample-size) scale, as well as a large-scale, in the formation of brachinites. At the least, it shows evidence of internal reduction itself, and at the most it shows us that there is evidence for internal reduction in other samples as well. Such evidence would support the interpretation that the redox relationship among bulk brachinites was established in a parent body setting. Nevertheless, we echo the caution of Mittlefehldt et al. (2003) that there is no direct evidence as to the nature of the responsible redox agent.

Is NWA 1500 a Brachinite?

We return to the question of whether NWA 1500 should be classified as a brachinite. As discussed above, although oxygen isotope and many petrographic, mineral compositional, and bulk compositional characteristics of NWA 1500 are indistinguishable from those of the majority of brachinites, the reverse zoning in its olivine (not observed in any brachinites) is a significant difference. On the other hand, we have pointed out a number of ways in which brachinites themselves are petrologically and compositionally diverse. Considering this overall diversity, we suggest that NWA 1500 shows sufficient similarities to brachinites that it should be classified as such. This classification is further supported by the evidence of internal reduction within NWA 1500 and some brachinites, which suggests common petrogenetic processes. By similar arguments, we recommend that NWA 595 retains its classification as a brachinite.

Acknowledgments—We thank Mike Jercinovic, Burkhard Schulz-Dobrick, and Elvira Macsenaere-Riester for assistance with SEM and EMPA; Bernard Spettel for assistance for neutron activation analyses; Joseph Boesenberg, Martin Prinz, Paul Warren, Tony Irving, Luigi Folco, Mini Wadhwa, and Rainer Bartoschewitz for providing meteorite samples; Shigeko Togashi and John Craven for providing plagioclase standards for SIMS analyses; and Frank Wlotzka, Ed Scott, David Mittlefehldt, and Mini Wadhwa for helpful discussions. We greatly appreciate the comments of the Associate Editor Christine Floss, and of referees Gretchen Benedix, Jason Herrin, and Doug Rumble, all of which helped us to improve this manuscript. This work was supported by NASA grants NNG05GH72G and NNX08AG63G to Cyrena Goodrich and NNX07AI46G to Noriko Kita WiscSIMS is partly supported by NSF (EAR03-19230, EAR05-16725, EAR07-44079).

Editorial Handling—Dr. Christine Floss

REFERENCES

Andersen D. J., Lindsley D. H., and Davidson P. M. 1993. QUILF: A PASCAL program to assess equilibria among Fe-Mg-Mn-Ti oxides, pyroxenes, olivine, and quartz. *Computers & Geosciences* 19:1333–1350.

Bartoschewitz R., Wlotzka F., Clayton R. N., and Mayeda T. K. 2003. NWA 1500: The first basaltic ureilite? (abstract). *Meteoritics & Planetary Science* 38:A65.

Benedix G. K., McCoy T. J., Keil K., Bogard D. D., and Garrison D. H. 1998. A petrologic and isotopic study of winonaites: Evidence for early partial melting, brecciation, and metamorphism. *Geochimica et Cosmochimica Acta* 62:2535–2553.

Buening D. K. and Buseck P. R. 1973. Fe-Mg lattice diffusion in olivine. *Journal of Geophysical Research* 78:6852–6862.

Burroni A. and Folco L. 2008. Frontier Mountain meteorite specimens of the acapulcoite-lodranite clan: Petrography, pairing, and parent-rock lithology of an unusual intrusive rock. *Meteoritics & Planetary Science* 43:731–744.

Clayton R. N. and Kieffer S. W. 1991. Oxygen isotopic thermometer calibrations. In *Stable isotope geochemistry: A tribute to Samuel Epstein*, edited by Taylor H. P. Jr., O'Neil J. R., and Kaplan I. R. Geochemical Society (Special Publication No. 3). pp. 3–10.

Clayton R. N. and Mayeda T. K. 1996. Oxygen isotope studies of achondrites. *Geochimica et Cosmochimica Acta* 60:1999–2017.

Clayton R. N., Onuma N., Grossman L., and Mayeda T. K. 1977. Distribution of pre-solar component in Allende and other carbonaceous chondrites. *Earth and Planetary Science Letters* 34:209–224.

Clayton R. N., Mayeda T. K., Goswami J. N., and Olsen E. J. 1991. Oxygen isotope studies of ordinary chondrites. *Geochimica et Cosmochimica Acta* 55:2317–2337.

Connolly H. C. Jr., Zipfel J., Grossman J. N., Folco L., Smith C., Jones R. H., Righter K., Zolensky M., Russell S. S., Benedix G. K., Yamaguchi A., and Cohen B. A. 2006. The Meteoritical Bulletin, No. 90 (September). *Meteoritics & Planetary Science* 41:A1383–A1418.

Connolly H. C. Jr., Smith C., Benedix G., Folco L., Righter K., Zipfel J., Yamaguchi A., and Chennaoui Aoudjehane H. 2008. The Meteoritical Bulletin, No. 93 (March). *Meteoritics & Planetary Science* 43:A571–A632.

Day J. M. D., Ash R. D., Liu Y., Bellucci J. J., Rumble D. III., McDonough W. F., Walker R. J., and Taylor L. A. 2009. Early formation of evolved asteroidal crust. *Nature* 457:179–182.

Downes H., Mittlefehldt D. W., Kita N. T., and Valley J. W. 2008. Evidence from polymict ureilites for a disrupted and re-accreted single ureilite parent asteroid gardened by several distinct impactors. *Geochimica et Cosmochimica Acta* 72:4825–4844.

Dreibus G., Palme H., Rammensee W., Spettel B., Weckworth G., and Wänke H. 1982. Composition of Shergotty parent body: Further evidence of a two component model of planet formation (abstract). 13th Lunar and Planetary Science Conference. pp. 186–187.

Goodrich C. A. 1992. Ureilites: A critical review. *Meteoritics* 27:327–352.

Goodrich C. A. 1998. Brachinites: Residues from low degrees of melting of a heterogeneous parent body (abstract). *Meteoritics & Planetary Science* 33:A60–A61.

Goodrich C. A. and Delaney J. S. 2000. Fe/Mg-Fe/Mn relations of meteorites and primary heterogeneity of achondrite parent bodies. *Geochimica et Cosmochimica Acta* 64:149–160.

Goodrich C. A. and Righter K. 2000. Petrology of unique achondrite Queen Alexandra Range 93148: A piece of the pallasite (howardite-eucrite-diogenite?) parent body? *Meteoritics & Planetary Science* 35:521–535.

Goodrich C. A., Jones J. H., and Berkley J. L. 1987. Origin and evolution of the ureilite parent magmas: Multi-stage igneous activity on a large parent body. *Geochimica et Cosmochimica Acta* 51:2255–2274.

Goodrich C. A., Fioretti A. M., Tribaudino M., and Molin G. 2001. Primary trapped melt inclusions in olivine in the olivine-augite-orthopyroxene ureilite Hughes 009. *Geochimica et Cosmochimica Acta* 65:621–652.

Goodrich C. A., Wlotzka F., Ross D. K., and Bartoschewitz R. 2006. Northwest Africa 1500: Plagioclase-bearing monomict ureilite or ungrouped achondrite? *Meteoritics & Planetary Science* 41:925–952.

Goodrich C. A., Van Orman J. A., and Wilson L. 2007. Fractional melting and smelting on the ureilite parent body. *Geochimica et Cosmochimica Acta* 71:2876–2895.

Goodrich C. A., Fioretti A. M., and Van Orman J. A. 2009. Petrogenesis of augite-bearing ureilites Hughes 009 and FRO 90054/93008 inferred from melt inclusions in olivine, augite and orthopyroxene. *Geochimica et Cosmochimica Acta* 73:3055–3076.

Greenwood R. C., Franchi I. A., Gibson J. M., and Benedix G. K. 2007. Oxygen isotope composition of the primitive achondrites (abstract #2163). 38th Lunar and Planetary Science Conference. CD-ROM.

Grossman J. 1998. The Meteoritical Bulletin, No. 82. *Meteoritics & Planetary Science* 33:A221–A239.

Irving A. J. and Rumble D. III. 2006. Oxygen isotopes in Brachina, Sahara 99555 and NWA 1054 (abstract #5288). *Meteoritics & Planetary Science* 41:A84.

Irving A. J., Kuehner S. M., and Rumble D. III. 2005. Brachinite NWA 3151 and (?)brachinite NWA 595 (abstract #5213). *Meteoritics & Planetary Science* 40:A73.

Ito M. and Ganguly J. 2006. Diffusion kinetics of Cr in olivine and ^{53}Mn-^{53}Cr thermochronology of early solar system objects. *Geochimica et Cosmochimica Acta* 70:799–809.

Jacobsen B., Yin Q.-Z., Moynier F., Amelin Y., Krot A. N., Nagashima K., Hutcheon I. D., and Palme H. 2008. ^{26}Al-^{26}Mg and ^{207}Pb-^{206}Pb systematics of Allende CAIs: Canonical solar initial ^{26}Al/^{27}Al ratio reinstated. *Earth and Planetary Science Letters* 272:353–364.

Janssens M.-J., Hertogen J., Wolf R., Ebihara M., and Anders E. 1987. Ureilites: Trace element clues to their origin. *Geochimica et Cosmochimica Acta* 51:2275–2283.

Johnson J. E., Scrygmour J. M., Jarosewich E., and Mason B. 1977. Brachina meteorite—A chassignite from South Australia. *Records of the South Australia Museum* 17:309–319.

Kallemeyn G. W. and Warren P. H. 1994. Geochemistry of LEW 88774 and two other unusual ureilites (abstract). 25th Lunar and Planetary Science Conference. pp. 663–664.

Kimura M., Tsuchiyama A., Fukuoa T., and Iimura Y. 1992. Antarctic primitive achondrites, Yamato-74025, -75300, and -75305: Their mineralogy, thermal history, and the relevance to winonaite. *Proceedings of the NIPR Symposium on Antarctic Meteorites* 5:165–190.

Kita N. T., Nagahara H., Togashi S., and Morishita Y. 2000. A short duration of chondrule formation in the solar nebula: Evidence from ^{26}Al in Semarkona ferromagnesian chondrules. *Geochimica et Cosmochimica Acta* 64:3913–3922.

Kita N. T., Mostefaoui S., Liu Y. Z., Togashi S., and Morishita Y. 2003a. Application of high precision SIMS ^{26}Al-^{26}Mg analyses to the early solar system chronology. *Applied Surface Science* 203–204:806–809.

Kita N. T., Ikeda Y., Shimoda H., Morishita Y., and Togashi S. 2003b. Timing of basaltic volcanism in ureilite parent body inferred from the ^{26}Al ages of plagioclase-bearing clasts in DaG 319 polymict ureilite (abstract #1557). 34th Lunar and Planetary Science Conference. CD-ROM.

Kita N. T., Ushikubo T., Fu B., and Valley J. W. 2009. High precision SIMS oxygen isotope analyses and the effect of sample topography. *Chemical Geology* 264:43–57.

Kita N. T., Nagahara H., Tachibana S., Tomomura S., Spicuzza M. J., Fournelle J. H., and Valley J. W. 2010. High precision SIMS oxygen three isotope study of chondrules in LL3 chondrites: Role of ambient gas during chondrule formation. *Geochimica et Cosmochimica Acta* 74:6610–6635.

Kring D. A., Boynton W. V., Hill D. H., and Haag R. A. 1991. Petrologic description of Eagles Nest: A new olivine achondrite (abstract). *Meteoritics* 26:360.

LaTourrette T. and Wasserburg G. J. 1998. Mg diffusion in anorthite: Implications for the formation of early solar system planetesimals. *Earth and Planetary Science Letters* 158:91–108.

McCoy T. J., Keil K., Clayton R. N., Mayeda T. K., Bogard D. D., Garrison D. H., Huss G. R., Hutcheon I. D., and Wieler R. 1996. A petrologic, chemical, and isotopic study of Monument Draw and comparison with other acapulcoites: Evidence for formation by incipient partial melting. *Geochimica et Cosmochimica Acta* 60:2681–2708.

McCoy T. J., Keil K., Clayton R. N., Mayeda T. K., Bogard D. D., Garrison D. H., and Wieler R. 1997. A petrologic and isotopic study of lodranites: Evidence for early formation as partial melt residues from heterogeneous precursors. *Geochimica et Cosmochimica Acta* 61:623–637.

Misener D. J. 1974. Cation diffusion in olivine to 1400 °C and 35 kbar. In *Geochemical transport and kinetics*, edited by Hoffmann A. W., Giletti B. J., Yoder H. S. Jr., and Yund R. A. Washington, D.C.: Carnegie Institute of Washington. pp. 117–129.

Mittlefehldt D. W. and Hudon P. 2004. Northwest Africa 1500: Not a basaltic ureilite; Not even a ureilite (abstract). *Meteoritics & Planetary Science* 39:A69.

Mittlefehldt D. W., Lindstrom M. M., Bogard D. D., Garrison D. H., and Field S. W. 1996. Acapulco- and Lodran-like achondrites: Petrology, geochemistry, chronology, and origin. *Geochimica et Cosmochimica Acta* 60:867–882.

Mittlefehldt D. W., McCoy T. J., Goodrich C. A., and Kracher A. 1998. Non-chondritic meteorites from asteroidal bodies. In *Planetary materials*, edited by Papike J. J. Reviews in Mineralogy, vol.36. Washington, D.C.: Mineralogical Society of America. 195 p.

Mittlefehldt D. W., Bogard D. D., Berkley J. L., and Garrison D. H. 2003. Brachinites: Igneous rocks from a differentiated asteroid. *Meteoritics & Planetary Science* 38:1601–1625.

Miyamoto M. and Takeda H. 1993. Rapid cooling of pallasite: Comparison of chemical zoning with primitive achondrites. *Meteoritics* 28:404–405.

Miyamoto M. and Takeda H. 1994. Thermal history of lodranites Yamato 74357 and MAC 88177 as inferred from the chemical zoning of pyroxene and olivine. *Journal of Geophysical Research* 99:5669–5677.

Miyamoto M., Takeda H., and Toyoda H. 1985. Cooling history of some Antarctic ureilites. Proceedings, 16th Lunar and Planetary Science Conference, Part 1. *Journal of Geophysical Research* 90(Suppl.):D116–D122.

Miyamoto M., Furuta T., Fujii N., McKay D. S., Lofgren G. E., and Duke M. B. 1993. The Mn-Fe negative correlation in olivine in ALHA77257 ureilite. *Journal of Geophysical Research* 98:5301–5307.

Miyamoto M., Mikouchi T., and Arai T. 2002. Comparison of Fe-Mg interdiffusion coefficients in olivine. *Antarctic Meteorite Research* 15:143–151.

Nagahara H. 1992. Yamato-8002: Partial melting residue on the "unique" chondrite parent body. *Proceedings of the NIPR Symposium on Antarctic Meteorites* 5:191–223.

Nagahara H. and Ozawa K. 1986. Petrology of Yamato-791493, "lodranite": Melting, crystallization, cooling history, and relationship to other meteorites. *Memoirs of the National Institute of Polar Research Special Issue* 41:181–205.

Nehru C. E., Prinz M., and Delaney J. S. 1983. Brachina: A new type of meteorite, not a chassignite. Proceedings, 14th Lunar and Planetary Science Conference, Part 1. *Journal of Geophysical Research* 88:B237–B244.

Nehru C. E., Prinz M., Weisberg M. K., Ebihara M. E., Clayton R. N., and Mayeda T. K. 1996. A new brachinite and petrogenesis of the group (abstract). 27th Lunar and Planetary Science Conference. p. 943.

Papike J. J., Spilde M. N., Fowler G. W., Layne G. D., and Shearer C. K. 1995. The Lodran primitive achondrite: Petrogenetic insights from electron and ion microprobe analysis of olivine and orthopyroxene. *Geochimica et Cosmochimica Acta* 59:3051–3070.

Patzer A., Hill D. H., and Boynton W. V. 2004. Evolution and classification of acapulcoites and lodranites from a chemical point of view. *Meteoritics & Planetary Science* 39:61–85.

Petaev M. I., Barsukova L. D., Lipschutz M. E., Wang M.-S., Ariskin A. A., Clayton R. N., and Mayeda T. K. 1994. The Divnoe meteorite: Petrology, chemistry, oxygen isotopes and origin. *Meteoritics* 29:182–199.

Rankenburg K., Humayan M., Brandon A. D., and Herrin J. S. 2008. Highly siderophile elements in ureilites. *Geochimica et Cosmochimica Acta* 72:4642–4659.

Rubin A. E. 2006. Shock, post-shock annealing and post-annealing shock in ureilites. *Meteoritics & Planetary Science* 41:125–133.

Rumble D. III, Irving A. J., Bunch T. E., Wittke J. H., and Kuehner S. M. 2008. Oxygen isotopic and petrological diversity among brachinites NWA 4872, NWA 4874, NWA 4882 and NWA 4969 (abstract #1974). 34th Lunar and Planetary Science Conference. CD-ROM.

Russell S. S., Zipfel J., Grossman J. N., and Grady M. M. 2002. The Meteoritical Bulletin, No. 86. *Meteoritics & Planetary Science* 37:A157–A184.

Russell S. S., Zipfel J., Folco L., Jones R.., Grady M. M., McCoy T. J., and Grossman J. N. 2003. The Meteoritical Bulletin, No. 87. *Meteoritics & Planetary Science* 38:A204.

Ryder G. 1982. Siderophiles in the Brachina meteorite: Impact melting? *Nature* 299:805–807.

Scott E. R. D., Taylor G. J., and Keil K. 1993. Origin of ureilite meteorites and implications for planetary accretion. *Geophysical Research Letters* 20:415–418.

Shearer C. K., Papike J. J., Burger P. V., Karner J., Borg L., Gaffney A., Neal C., Shafer J., Fernandes V. A., Sharp Z., Weiss B. P., and Geissman J. 2008. GRA06129: A meteorite from a new asteroidal geochemical reserovir or Venus (abstract #1825)? 39th Lunar and Planetary Science Conference. CD-ROM.

Shearer C. K., Burger P. V., Neal C., Sharp Z., Spivak-Birndorf L., Borg L., Fernandes V. A., Papike J. J., Karner J., Wadhwa M., Gaffney A., Shafer J., Geissman J., Atudorei N.-V., Herd C., Weiss B. P., King P. L., Crowther S. A., and Gilmour J. D. 2010. Non-basaltic asteroidal magmatism during the earliest stages of solar system evolution: A view from Antarctic achondrites Graves Nunatak 06128 and 06129. *Geochimica et Cosmochimica Acta* 74:1172–1199.

Smith J. V., Steele I. M., and Leitch C. A. 1983. Mineral chemistry of the shergottites, nakhlites, Chassigny, Brachina, pallasites, and ureilites. Proceedings, 14th Lunar and Planetary Science Conference, Part. 1. *Journal of Geophysical Research* 88:B229–B236.

Spicuzza M. J., Day J. M. D., Taylor L. A., and Valley J. W. 2007. Oxygen isotope constraints on the origin and differentiation of the Moon. *Earth and Planetary Science Letters* 253:254–265.

Swindle T. D., Kring D. A., Burkland M. K., Hill D. H., and Boynton W. V. 1998. Noble gases, bulk chemistry, and petrography of olivine-rich achondrites Eagles Nest and Lewis Cliff 88763: Comparison to brachinites. *Meteoritics & Planetary Science* 33:31–48.

Takeda H. 1987. Mineralogy of Antarctic ureilites and a working hypothesis for their origin and evolution. *Earth and Planetary Science Letters* 81:358–370.

Takeda H. 1989. Mineralogy of coexisting pyroxenes in magnesian ureilites and their formation conditions. *Earth and Planetary Science Letters* 93:181–194.

Takeda H., Mori H., and Ogata H. 1989. Mineralogy of augite-bearing ureilites and the origin of their chemical trends. *Meteoritics* 24:73–81.

Takeda H., Mori H., Hiroi T., and Saito J. 1994. Mineralogy of new Antarctic achondrites with affinity to Lodran and a model of their evolution in an asteroid. *Meteoritics* 29:830–842.

Treiman A. H., Drake M. J., Janssens M.-J., Wolf R., and Ebihara M. 1986. Core formation in the earth and shergottite parent body (SPB): Chemical evidence from basalts. *Geochimica et Cosmochimica Acta* 50:1071–1091.

Valley J. W., Kitchen N., Kohn M. J., Niendorf C. R., and Spicuzza M. J. 1995. UWG-2, a garnet standard for oxygen isotope ratios: Strategies for high precision and accuracy with laser heating. *Geochimica et Cosmochimica Acta* 59:5223–5231.

Wadhwa M., Zipfel J., and Davis A. M. 1998a. Constraints on the formation history of brachinites from rare-earth-element distributions (abstract). *Meteoritics & Planetary Science* 33:A161.

Wadhwa M., Shukolyukov A., and Lugmair G. 1998b. ^{53}Mn-^{53}Cr systematics in Brachina: A record of one of the earliest phases of igneous activity on an asteroid (abstract

#1480). 29th Lunar and Planetary Science Conference. CD-ROM.
Warren P. H. and Kallemeyn G. W. 1989. Allan Hills 84025: The second brachinite, far more differentiated than Brachina, and an ultramafic achondritic clast from L chondrite Yamato 75097. Proceedings, 19th Lunar and Planetary Science Conference. pp. 475–486.
Warren P. H. and Kallemeyn G. W. 1992. Explosive volcanism and the graphite-oxygen fugacity buffer on the parent asteroid(s) of the ureilite meteorites. *Icarus* 100:110–126.
Warren P. H., Ulff-Møller F., Huber H., and Kallemeyn G. W. 2006. Siderophile geochemistry of ureilites; a record of early stages of planetesimal core formation. *Geochimica et Cosmochimica Acta* 70:2104–2126.
Weber I., Bischoff A., and Weber D. 2003. TEM investigations on the monomict ureilites Jalanash and Hammadah al Hamra 064. *Meteoritics & Planetary Science* 38:145–156.
Weisberg M. K., McCoy T. J., and Krot A. N. 2006. Systematics and evaluation of meteorite classification. In *Meteorites and the early solar system, II*. pp. 19–52.
Weisberg M. K., Smith C., Benedix G., Folco L., Righter K., Zipfel J., Yamaguchi A., and Chennaoui Aoudjehane H. 2008. The Meteoritical Bulletin, No. 94 (September). *Meteoritics & Planetary Science* 43:A1551–A1588.
Wilson L. W., Goodrich C. A., and Van Orman J. A. 2008. Thermal evolution and physics of melt extraction on the ureilite parent body. *Geochimica et Cosmochimica Acta* 72:6154–6176.
Wlotzka F. 1972. Havero ureilite: Evidence for recrystallization and partial reduction. *Meteoritics* 7:591–600.
Wlotzka F. 1993a. A weathering scale for the ordinary chondrites (abstract). *Meteoritics* 280:460.
Wlotzka F. 1993b. The Meteoritical Bulletin, No. 75. *Meteoritics* 28:A692–A703.
Meteoritical Bulletin Database. http://tin.er.usgs.gov/meteor/index.php.
Yugami K., Takeda H., Kojima H., and Miyamoto M. 1998. Modal mineral abundances and the differentiation trends in primitive achondrites. *Antarctic Meteorite Research* 11:49–70.
Zeigler R. A., Jolliff B. L., Korotev R. L., Rumble D., III., Carpenter P. K., and Wang A. 2008. Petrology, geochemistry and likely provenance of unique achondrite Graves Nunataks 06128 (abstract #2456). 39th Lunar and Planetary Science Conference. CD-ROM.

SUPPORTING INFORMATION

Additional Supporting Information may be found in the online version of this article:

Table S1. SIMS oxygen isotope analyses of standards and NWA 1500, showing both raw and corrected data in the order of analysis sequence.

Table S2. Al-Mg isotope analyses of standard and NWA 1500 plagioclase.

Table S3. Equilibrium oxygen isotope fractionation between olivine and plagioclase.

Please note: Wiley-Blackwell is not responsible for the content or functionality of any supporting materials supplied by the authors. Any queries (other than missing material) should be directed to the corresponding author for the article.